Mechanism of Oxidative Cleavage of Organocobalt(III) Macrocycles. Application of Electrochemical Techniques to Irreversible Electron-Transfer Processes

W. H. Tamblyn, R. J. Klingler, W. S. Hwang, and J. K. Kochi*

Contribution from the Department of Chemistry, Indiana University, Bloomington, Indiana 47401. *Received July 18, 1980*

Abstract: The thermally stable dimethylcobalt(III) macrocycles, *trans*-$Me_2Co(DpnH)$ and *trans*-$Me_2Co(TIM)ClO_4$, are strongly labilized upon chemical and electrochemical oxidation, leading to the selective scission of only one methyl ligand. The formation of highly labile dimethylcobalt(IV) cations as reactive intermediates is evident from the irreversibility of the cyclic voltammetric (CV) wave even at −78 °C. The heterogeneous rates of electron transfer are obtained from the CV data and compared with the corresponding homogeneous rates measured with various polypyridineiron(III) and hexachloroiridate(IV) oxidants. The resulting linear correlation underscores a common outer-sphere mechanism for the primary steps in the electrochemical and chemical oxidations. The cleaved methyl ligand affords ethane in high yields, but it can be trapped by hydrogen atom donors (chloroform) as methane and by halogen atom donors (carbon tetrachloride and benzyl bromide) as methyl halides. The kinetic study of ethane formation by a competition method supports the mechanism in Scheme III, in which the spontaneous homolytic fragmentation of the dimethylcobalt(IV) intermediate leads to a free methyl radical. The subsequent diffusive encounter of methyl radicals is in accord with the deuterium-labeling study which establishes a pattern of random dimerization of methyl ligands. The alternative formulation involving the direct bimolecular reaction of a pair of dimethylcobalt(IV) cations is ruled out by the insensitivity of ethane formation to the ionic strength of the medium. Methyl radical as the active precursor also follows from the selectivity pattern (observed in the competitive trapping with halogen atom donors), which is identical with that of the methyl radical generated independently from the photolysis of acetyl peroxide. A complete kinetic analysis of this mechanistic scheme provides information about the lifetime of the metastable dimethylcobalt(IV) species at the electrode surface which is sufficient to generate a high flux of methyl radicals to ensure efficient dimerization.

Interest in the alkylcobalt(III) complexes, especially those with macrocyclic quadridentate ligands related to the biologically important corrin, stems in part from the large variety of structural types with exceedingly stable carbon-to-metal bonds.[1] Moreover, the ability of the synthetic models to stabilize the cobalt center in the formal oxidation states—Co(I), Co(II), Co(III), and Co(IV)—offers an opportunity for examining the redox chemistry of this important class of organometallic compounds.

The oxidative cleavage of the monoalkylcobalt(III) complexes of dimethylglyoxime (cobaloximes) has been extensively investigated.[2] The two types of cobalt(III) macrocyclic chelates examined in this study, viz., chelate = DpnH and TIM,[3] are formally related to the cobaloximes, and they all differ in the overall charge in the complex, i.e.,

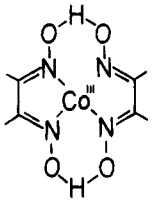

$Co(DMG)_2^+$

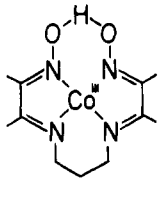

$Co(DpnH)^{2+}$

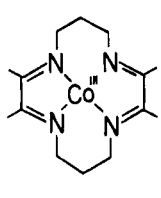

$Co(TIM)^{3+}$

A wide variety of the monoalkyl derivatives of these cobalt(III) macrocycles have been synthesized, but the dialkyl analogues are only known for $Co(DpnH)^{2+}$ and $Co(TIM)^{3+}$.

Table I. Cyclic Voltammetric Data for Dimethylcobalt(III) and Alkylcobalt(III) Macrocyclic Complexes[a]

organocobalt(III) macrocycle	E_p,[b] V	β[c]	$i_p/Cv^{1/2}$ [d]
$Me_2Co(DpnH)$	0.43[e]	0.77	1.7
$Me_2Co(TIM)^+$	0.32[e]	0.61	1.8
$MeCo(DpnH)(H_2O)^+$	1.57[f]	0.62	
$EtCo(DpnH)(H_2O)^+$	1.43[f]	0.78	2.2
n-$PrCo(DpnH)(H_2O)^+$	1.55[f]	0.64	2.0
$Co(DpnH)Cl_2$	2.07	0.58	1.6

[a] Measured with a scan rate of 100 mV s^{-1} at 25 °C in a 5 × 10^{-3} M organocobalt(III) complex in acetonitrile containing 0.1 M Et_4NClO_4. [b] Anodic peak potential; voltage relative to saturated NaCl-SCE. [c] Transfer coefficient determined from the width of the anodic wave (see Experimental Section). [d] Current function in units of mA M^{-1} $(mV/s)^{-1/2}$. [e] Calibrated with 1,4-benzoquinone internal standard. [f] Internal ferrocene standard, employed for the accuracy of the potential measurements.

The electrochemical oxidation of the monoalkylcobaloximes and related Schiff's base complexes proceeds by a reversible one-electron process to afford relatively stable alkylcobalt(IV) species in which the alkyl ligands are subject to nucleophilic displacement.[2] By contrast, we wish to show that the anodic electrochemistry of the dimethylcobalt(III) macrocycles is highly irreversible and leads to transient dimethylcobalt(IV) species, whose mechanistic fate is one of the principal objectives of this study. More generally, however, we wish to exploit the dimethylcobalt(III) macrocycles to demonstrate how the combined application of electrochemical and chemical probes can lead to the elucidation of mechanisms which involve intermediates too transient to be seen by standard electrochemical means alone.[4,5]

(1) For reviews see: (a) Dodd, D.; Johnson, M. D. *J. Organomet. Chem.* **1973**, *52*, 2. (b) Witman, M. W.; Weber, J. H. *Inorg. Chem. Acta* **1977**, *23*, 263. (c) For a recent electrochemical study of vitamin B_{12} and derivatives, see: Lexa, D.; Savéant, J. M.; and Zickler, J. *J. Am. Chem. Soc.* **1980**, *102*, 2654, 4852.

(2) (a) Abley, P.; Dockal, E. R.; Halpern, J. *J. Am. Chem. Soc.* **1972**, *94*, 659. (b) Halpern, J.; Chan, M. S.; Hanson, J.; Roche, T. S.; Topich, J. A. *Ibid.*, **1975**, *97*, 1606. (c) Magnuson, R. H.; Halpern, J.; Levitin, I. Ya.; Vol'pin, M. E. *Chem. Commun.* **1978**, 44; *J. Organomet. Chem.* **1976**, *114*, C53. (d) Halpern, J.; Topich, J.; Zamaraev, K. I. *Inorg. Chim. Acta* **1976**, *20*, L21. (e) Topich, J.; Halpern, J. *Inorg. Chem.* **1979**, *18*, 1339.

(3) DpnH = 2,3,9,10-tetramethyl-1,4,8,11-tetraazaundeca-1,3,8,10-tetraen-11-ol-1-olate; TIM = 2,3,9,10-tetramethyl-1,4,8,11-tetraazacyclotetradeca-1,3,8,10-tetraene.

(4) (a) Pletcher, D. *Chem. Soc. Rev.* **1975**, *75*, 1190. (b) Streitweiser, A. In "Physical Methods in Chemistry"; Weissberger, A.; Rossiter, B. W., Eds.; Wiley-Interscience: New York, 1971; Part IIa. (c) Saveant, J. M.; Vianello, E. *C. R. Hebd. Seances Acad. Sci.* **1963**, *256*, 2597; (d) Nicholson, R. S.; Shain, I. *Anal. Chem.* **1964**, *36*, 706.

(5) (a) Baizer, M. Ed. "Organic Electrochemistry"; Marcel Dekker: New York, 1969. (b) Adams, R. N. "Electrochemistry at Solid Electrodes"; Marcel Dekker: New York, 1969.

0002-7863/81/1503-3161$01.25/0

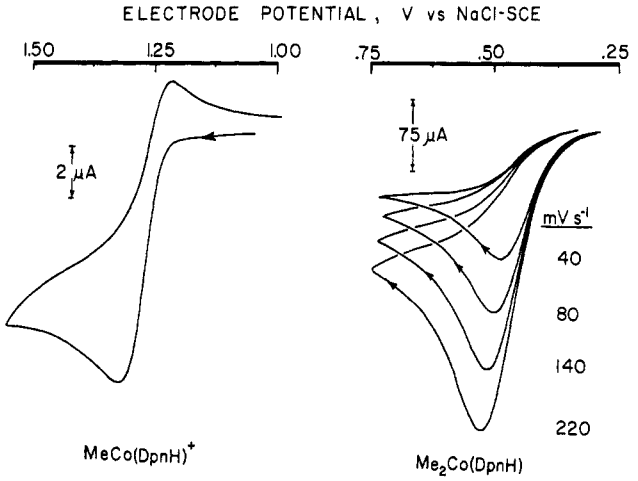

Figure 1. Left: First scan cyclic voltammogram of 2.2×10^{-3} M $MeCo(DpnH)ClO_4$ in *n*-butyronitrile containing 0.2 M tetrabutylammonium perchlorate at −92 °C with a scan rate of 40 mV s^{-1}. Right: CV of 6.0×10^{-3} M $Me_2Co(DpnH)$ in acetonitrile solution containing 0.1 M TEAP at 25 °C with the use of various scan rates.

Results

The anodic electrochemistry and the chemical oxidation of the *trans*-dimethylcobalt(III) macrocycles—the neutral $Me_2Co(DpnH)$ and the cationic $Me_2Co(TIM)^+$—were the primary objectives of this study. However, the monoalkylcobalt(III) analogues, $RCo(DpnH)^+$, where R = methyl, ethyl, and *n*-propyl, were also examined for comparative purposes.

I. Cyclic Voltammetry of *trans*-Dimethylcobalt(III) Macrocycles. The single sweep cyclic voltammogram (CV) of the various alkyl-substituted cobalt(III) macrocyclic complexes listed in Table I was recorded with a stationary platinum microelectrode at 25 °C in acetonitrile solutions containing 0.1 M tetraethylammonium perchlorate (TEAP). Each of the complexes exhibited a well-defined anodic wave, but no cathodic process was detected on the reverse scan, even at sweep rates as high as 10 V s^{-1}, indicative of the existence of a fast and irreversible follow-up chemical process. Reducing the temperature was of limited utility in slowing down the subsequent decomposition. Although some reversibility was evident when a solution of the monomethyl derivative $MeCo(DpnH)^+$ was cooled to −92 °C, as illustrated in Figure 1 (left), neither of the dimethyl analogues $Me_2Co(DpnH)$ nor $Me_2Co(TIM)^+$ showed any signs of such reversibility even at these low temperatures. Further evidence of the rapidity of the follow-up chemical process can be gained by the analysis of the sweep dependence of the anodic wave. Thus Figure 1 (right) reveals that the current in the foot of the wave is singularly independent of the sweep rate. This behavior, originally noted by Reinmuth,[6] could indicate that the forward electron-transfer step is totally irreversible, i.e., electron transfer proceeds only in the forward direction. Such a situation would result if the oxidized alkylcobalt(IV) cation were unstable and any follow-up chemical process leading to decomposition became faster then the reverse electron transfer to regenerate the alkylcobalt(III) complex.[7-9] We have applied a number of other more rigorous electrochemical criteria to establish that the electrochemical process is not reversible, as described in detail in the Experimental Section. Suffice to emphasize here that the oxidized alkylcobalt(IV) cation is sufficiently transient to compete effectively with the reverse electron-transfer process. Indeed, independent measurements employing double-step chronoamperometry limits its lifetime to less than 1 ms. No deterioration of the electrode response was observed upon repeated CV scans, indicative of an anodic oxidation which cleanly leads to products without fouling the electrode surface.

Table II. Stoichiometry of the Electrochemical and Chemical Oxidation of Dimethylcobalt(III) Macrocycles[a]

dimethylcobalt(III) macrocycle	oxidant	equiv oxidant per $Me_2Co(III)$ titration[b]	prod[c]
$Me_2Co(DpnH)$	electrochem	1.05[d]	
$Me_2Co(DpnH)$	$Fe(phen)_3(ClO_4)_3$	1.06	0.91
$Me_2Co(DpnH)$	$Fe(5\text{-Cl-phen})_3(ClO_4)_3$	1.05	0.98
$Me_2Co(DpnH)$	$Cu(O_3SCF_3)_2$		0.99
$Me_2Co(DpnH)$	$Fe(bpy)_3(ClO_4)_3$	1.11[e]	1.05[e]
$Me_2Co(DpnH)$	Na_2IrCl_6	1.61	1.96
$Me_2Co(TIM)^+$	electrochem	1.06[f]	
$Me_2Co(TIM)^+$	$Fe(phen)_3(ClO_4)_3$		1.16

[a] In acetonitrile solution containing 2–4 × 10^{-3} M $Me_2Co(III)$ at 25 °C. [b] Spectral titration from the break in the absorbance at 510 nm. [c] Chemical titration by using the following molar absorptivities: $Fe(phen)_3^{3+}$, 1.30×10^4 M^{-1} cm^{-1} (507 nm); $Fe(5\text{-Cl-phen})_3^{3+}$, 9.33×10^3 M^{-1} cm^{-1} (510 nm); $Fe(bpy)_3^{3+}$, 8.24×10^3 M^{-1} cm^{-1} (520 nm); $Me_2Co(DpnH)$, 7.28×10^3 M^{-1} cm^{-1} (510 nm). [d] From coulometry at $E = 0.45$ V vs. NaCl-SCE. [e] Under 1 atm of O_2. [f] From coulometry at 0.35 V vs. NaCl-SCE.

II. Stoichiometry and Products of the Oxidation of Dimethylcobalt(III) Macrocycles. A. Coulometry and Spectral Titration. Bulk electrolysis at a platinum gauze electrode of a 10^{-2} M acetonitrile solution of either $Me_2Co(DpnH)$ or $Me_2Co(TIM)^+$ at the CV peak potential E_p resulted in the passage of 1.05 ± 0.05 faraday of charge per dimethylcobalt(III) complex, in accord with the oxidation in eq 1. The coulometric *n* value

$$Me_2Co(DpnH) \rightarrow Me_2Co(DpnH)^+ + e^- \quad (1)$$

of 1 is also consistent with the stoichiometry of the chemical oxidation of the same complexes with the various iron(III) and copper(II) oxidants listed in Table II, e.g.,

$$Me_2Co(DpnH) + Fe(phen)_3^{3+} \rightarrow Me_2Co(DpnH)^+ + Fe(phen)_3^{2+} \quad (2)$$

The stoichiometries of the oxidation were determined by both spectral titrimetric methods and product stoichiometry, as described in the Experimental Section. In contrast to these oxidants, 2 equiv of hexachloroiridate(IV) were required for the oxidation of the dimethylcobalt(III) complexes (vide infra).

B. Products. The electrochemical as well as the chemical oxidation of dimethylcobalt(III) macrocycles result quantitatively in the selective loss of only one methyl ligand to produce the monomethylcobalt(III) cation according to the stoichiometry in eq 3. The monomethylcobalt complexes were identified by

$$Me_2Co(DpnH) + Fe(phen)_3^{3+} \rightarrow MeCo(DpnH)^+ + [CH_3] + Fe(phen)_3^{2+} \quad (3)$$

comparing their ^1H NMR spectra and thin layer chromatographic behavior with those of authentic samples of $MeCo(DpnH)(H_2O)(ClO_4)$ and $MeCo(TIM)(H_2O)(ClO_4)_2$.

The fate of the cleaved methyl group (represented as $[CH_3]$ in eq 3) is highly dependent on the experimental conditions. Thus, the cleaved methyl group was accounted for principally as ethane together with lesser amounts of methane, when the oxidative cleavages of the dimethylcobalt(III) complexes were carried out either anodically at the CV peak potential E_p or chemically with the following oxidants, $Cu(O_3SCF_3)_2$, $Ag(O_3SCF_3)$, $Fe(phen)_3(ClO_4)_3$, $Fe(bpy)_3(ClO_4)_3$, $Fe(5\text{-Cl-phen})_3(ClO_4)_3$, and $Ce(NO_3)_6(NH_4)_2$, as listed in Table VII of the Experimental Section. It is noteworthy that the yield of methane increases monotonically at the expense of ethane when the controlled potential bulk

(6) Reinmuth, W. H. *Anal. Chem.* **1960**, *32*, 1891.
(7) See ref 8c for a detailed theoretical description of the various kinetic possibilities which have been graphically represented by "kinetic zone" diagrams. See also ref 9 for a recent application of these principles to the oxidation of a series of alkylmetals of the main group elements.
(8) (a) Delahay, P. *J. Am. Chem. Soc.* **1053**, *75*, 1190. (b) Nicholson, R. S.; Shain, I. *Anal. Chem.* **1964**, *36*, 706. (c) Nadjo, L.; Saveant, J. M. *Electroanal. Chem.* **1973**, *48*, 113. (d) Matsuda, H.; Ayabe, Y. *Z. Elektrochem.* **1955**, *59*, 494.
(9) Klingler, R. J.; Kochi, J. K. *J. Am. Chem. Soc.* **1980**, *102*, 4790.

Table III. Observed and Calculated Mass Spectra of the Ethane Produced in the Oxidation of Various Mixtures of $(CH_3)_2Co(DpnH)$ and $(CD_3)_2Co(DpnH)$[a]

	oxidant[$(CH_3)_2Co/(CD_3)_2Co$]							
	$Fe(phen)_3(ClO_4)_3$ [1.0/1.0]		$Cu(O_3SCF_3)_2$ [1.0/1.0]		$Fe(phen)_3(ClO_4)_3$ [0.3/0.7]		$Fe(phen)_3(ClO_4)_3$ [0.7/0.3]	
m/e	obsd[b]	calcd[c]	obsd[b]	calcd[c]	obsd[b]	calcd[d]	obsd[b]	calcd[e]
36	8.7	(8.9)	8.4	(8.9)	19.1	(19.0)	2.2	(3.3)
34	6.1	(5.9)	6.0	(5.9)	12.8	(12.6)	2.1	(2.2)
33	24.6	(24.9)	23.5	(24.9)	23.1	(24.4)	16.6	(21.6)
32	48.9	(50.8)	45.3	(50.8)	88.4	(95.0)	18.2	(24.9)
31	18.6	(17.0)	18.5	(17.0)	18.8	(18.3)	13.6	(15.0)
30	100	(100)	100	(100)	100	(100)	84.0	(99.0)
29	33.1	(30.3)	31.5	(30.3)	25.3	(23.7)	35.0	(35.8)
28	71.6	(65.1)	67.9	(65.1)	46.4	(50.0)	100	(100)
27	28.1	(28.0)	27.9	(28.0)	17.0	(18.3)	37.6	(41.1)
26	16.5	(14.6)	15.0	(14.6)	9.4	(10.2)	22.2	(23.2)
25	3.4		3.2		1.7		4.3	
24	1.2		1.0					
18	3.6	(3.7)	2.9	(3.7)	4.6	(5.9)	1.5	(2.3)
16	2.1		2.2		3.3		1.1	
15	3.2	(3.6)	3.0	(3.6)	1.9	(2.6)	3.8	(4.7)
14	2.9		2.9		2.5		2.9	

[a] In acetonitrile solutions at 25 °C. [b] The intensities normalized to 100 for the largest peak. [c] The calculated values based on statistical scrambling are in parentheses. D_0, D_3, and D_6 calculated on the basis of 1:2:1. [d] D_0, D_3, and D_6 calculated on the basis of 0.09:0.42:0.49. [e] D_0, D_3, and D_6 calculated on the basis of 0.49:0.42:0.09.

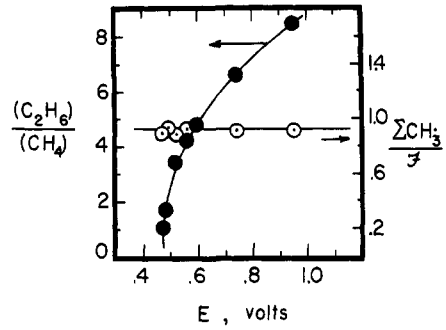

Figure 2. Potential dependence of the relative yields of ethane and methane (●) from the anodic oxidation of 10^{-2} M $Me_2Co(DpnH)$ in acetonitrile containing 0.1 M TEAP at 25 °C. Right scale ⊙ shows the constancy of the total yield of the cleaved methyl group (as CH_4 plus $2C_2H_6$) per Faraday of charge.

electrolysis is performed at potentials progressively less positive than E_p. Indeed, the molar ratio of ethane to methane shows an exponential dependence on the applied potential in Figure 2, while maintaining the yield of the cleaved methyl group to a consistent stoichiometry of 1 equiv per faraday of charge passed. Such an observed potential dependence of the volatile reaction products cannot be accounted for by a simple first-order decomposition of a transient intermediate such as the cationic $Me_2Co(DpnH)^+$, as described later (vide infra).

When hexachloroiridate(IV) is the oxidant, the cleaved methyl ligand is quantitatively accounted for as methyl chloride in Table VII, with only traces of ethane and methane. The formal oxidation of the methyl ligand according to eq 4 accords with the stoi-

$$Me_2Co(DpnH) + 2IrCl_6^{2-} \xrightarrow[CH_3CN]{} MeCo(DpnH)^+ + MeCl + IrCl_6^{3-} + IrCl_5(CH_3CN)^{2-} \quad (4)$$

chiometric requirement of two $IrCl_6^{2-}$ reported in Table II for this oxidant.[10]

C. Deuterium-Labeling Studies. In order to differentiate between an intramolecular and an intermolecular route for ethane formation, various mixtures of $(CH_3)_2Co(DpnH)$ and $(CD_3)_2Co(DpnH)$ were chemically oxidized and the isotopically labeled ethane was analyzed by mass spectrometry.[11] The ex-

(10) For a related study of alkylplatinum complexes see: Chen, J. Y.; Kochi, J. K. *J. Am. Chem. Soc.* **1977**, *99*, 1450.

(11) For additional details see Tamblyn, W. H., Ph.D. Dissertation, Indiana University.

Table IV. Rate Constants for the Heterogeneous (k_e) and Homogeneous (k_h) Oxidation of Various Organocobalt(III) Macrocycles[a]

organocobalt(III) macrocycle	oxidant	k_h, M^{-1} s^{-1}	k_e, cm s^{-1} [d]
1. $Me_2Co(DpnH)$	Na_2IrCl_6	4.0×10^2	1.9×10^{-2}
2. $Me_2Co(TIM)^+$	Na_2IrCl_6	2.8×10^3	2.0×10^{-1}
3. $Me_2Co(DpnH)$	$Fe(bpy)_3^{3+}$	$>10^6$ [b]	1.7×10^5
4. $MeCo(DpnH)^+$	$Fe(5\text{-}NO_2\text{-}phen)_3^{3+}$	2.9	1.2×10^{-6}
5. $MeCo(DpnH)^+$	$Fe(phen)_3^{3+}$	1.6×10^{-2}	1.1×10^{-8}
6. $EtCo(DpnH)^+$	$Fe(bpy)_3^{3+}$	3.0×10^{-1}	1.7×10^{-8}
7. $EtCo(DpnH)^+$	$Fe(5\text{-}NO_2\text{-}phen)_3^{3+}$	5.4×10^2	8.0×10^{-6}
8. $EtCo(DpnH)^+$	Na_2IrCl_6	*c*	1.6×10^{-15}

[a] In acetonitrile solution containing 0.1 M $NaClO_4$ or TEAP at 25 °C, using 10^{-3}–10^{-5} M organocobalt(III) complexes and 10^{-3}–10^{-5} M oxidants. [b] Rate too fast to measure reliably by stopped-flow methods. [c] Rate too slow to observe within 24-h period; $k_h < 10^{-6}$ M^{-1} s^{-1}. [d] Obtained from eq 13 and the data in Table I (see Discussion). Note: $k(E) = k_e$ at $E = E^0$ of the oxidant, as cited in ref 21.

cellent agreements shown in Table III between the measured intensities and the mass spectra, calculated on the basis of statistical scrambling, provide conclusive proof that ethane is produced in an intermolecular process, involving the random coupling of methyl groups. (For clarity, the macrocyclic ligand is omitted from the presentation in eq 5 and in the following equations.)

$$(CH_3)_2Co^{III} + (CD_3)_2Co^{III} \xrightarrow{\text{(oxidation)}} CH_3CH_3,\ CH_3CD_3,\ CD_3CD_3,\ \text{etc.} \quad (5)$$

III. Kinetics of the Oxidation of Dimethylcobalt(III) Macrocycles with Iron(III) and Iridium(IV) Oxidants in Solution. The rates of the homogeneous chemical oxidation of $Me_2Co(DpnH)$ and $Me_2Co(TIM)^+$ with a series of polypyridineiron(III) and hexachloroiridate(IV) complexes listed in Table IV, were examined in acetonitrile solutions at 25 °C. The oxidation of the dimethylcobalt(III) complexes with hexachloroiridate(IV) was measured spectrophotometrically with the use of a Durrum-Gibson stopped-flow spectrophotometer. The reaction obeyed overall second-order kinetics, being first order in each reactant according to eq 6. The oxidation of the monoalkylcobalt(III) species

$$\frac{-d[Me_2Co^{III}]}{dt} = k_h[Me_2Co^{III}][Na_2IrCl_6] \quad (6)$$

$EtCo(DpnH)^+$ with hexachloroiridate(IV) was too slow to measure accurately, the rate constant being estimated as less than 10^{-6} M^{-1}

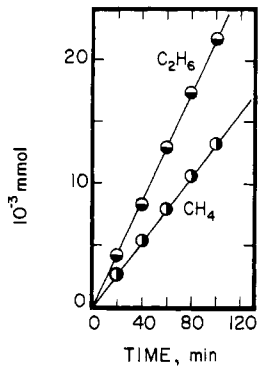

Figure 3. Rate of ethane and methane formation during the anodic oxidation of 1.0×10^{-2} M $Me_2Co(DpnH)$ in acetonitrile with 0.1 M TEAP at 25 °C under a constant current of 1.0 mA.

s^{-1}. However, the oxidation could be effected with various tris(phenanthroline)iron(III) complexes, and the second-order rate constants for these oxidations are also listed in Table IV.

IV. The Kinetics of Ethane Formation during the Electrooxidation of Dimethylcobalt(III) Macrocycles. Since the cyclic voltammograms in Figure 1 are not characteristic of electrochemically reversible processes, the standard analysis based on the shift of the peak potential with scan rate[4] cannot be used to obtain kinetic information on the subsequent chemical reactions, particularly those leading to ethane. Thus in order to determine the route by which ethane is formed during electrooxidation, the kinetic dependence on the dimethylcobalt(III) macrocycle was determined by chemical trapping techniques. The identity of the active radical precursor was then examined by the use of selectivity studies in halogen atom transfer and by variations of the ionic strengh of the medium.

A. The Effect of Dimethylcobalt(III) Concentration on the Rate of Ethane Formation. The yields of ethane and methane both increase linearly with time, when the anodic oxidation of $Me_2Co(DpnH)$ is carried out at a platinum gauze electrode at constant current, as shown in Figure 3. [Note: For analytical purposes, these electrolyses were carried out at potentials more negative than E_p to accentuate methane formation (see Figure 2). The level of the applied current in these experiments cannot be sustained past a 50% conversion of the dimethylcobalt(III) macrocycle, owing to its low concentration at the electrode surface during the later stages of the electrolysis.] The results suggest that the rate of formation of the gaseous products is determined by the rate of oxidation. Moreover the rate of product formation must be independent of the concentration of the unoxidized dimethylcobalt(III) macrocycle, which is falling off exponentially within the Nernst diffusion layer as the electrolysis proceeds. In order to establish this point more fully, the kinetics of ethane formation were measured by the competition method since it is too fast to be directly measured by conventional techniques.

For the competition study, two structurally distinct types of chemical traps XY were employed to monitor the ethane formation—namely, an active hydrogen atom source (chloroform) and a halogen atom source (carbon tetrachloride and benzyl bromide), i.e.,

$$Me_2Co(DpnH)^+ \rightarrow CH_3CH_3, \text{ etc.} \quad (7)$$

$$Me_2Co(DpnH)^+ \xrightarrow{XY} CH_3X, \text{ etc.} \quad (8)$$

where X–Y = H–CCl_3, Cl–CCl_3, and Br–CH_2Ph. The anodic oxidations were carried out at a constant current, the level of which was chosen not to exceed 10% of the limiting current.[12] [In this way we could be assured that the concentration of the electroactive dimethylcobalt(III) macrocycle within the Nernst diffusion layer was not significantly different from that in the bulk solution.] The electrolysis was carried out to less than 10% conversion, and the resultant organic products were analyzed quantitatively by gas chromatography. The results with chloroform in Figure 4a clearly indicate that the cleaved methyl groups can be trapped as methane, which is shown to increase linearly with the chloroform concentration.[13] It is noteworthy that this plot (obtained after subtraction of the background methane which is formed in the absence of chloroform) passes through the origin. Similar results are shown in Figure 4b, in which the cleaved methyl groups are trapped as methyl chloride by carbon tetrachloride. Finally, benzyl bromide is seen to be both a bromine atom donor (methyl bromide) as well as a hydrogen atom donor (methane) in Figure 4c. The trichloromethyl group derived from the chloroform and carbon tetrachloride traps was accounted for as the dimeric hexachloroethane.

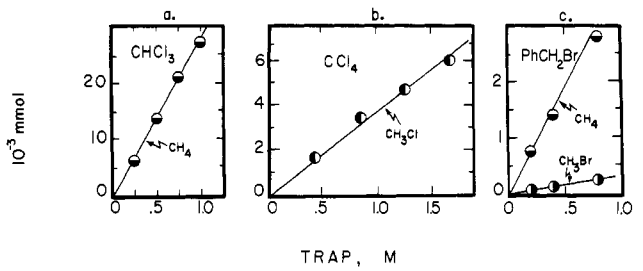

Figure 4. Chemical trapping of the cleaved methyl ligand during the electrooxidation of 1.0×10^{-2} M $Me_2Co(DpnH)$ in the presence of various amounts of (a) chloroform to form methane (◒), (b) carbon tetrachloride to form methyl chloride (◐), and (c) benzyl bromide to form methyl bromide (◑) and methane (◒). Background methane corrected for in (a) and (c).

Table V. Kinetic Dependence of Ethane Formation on the Concentration of $Me_2Co(DpnH)$ during Electrooxidation at Constant Current[a]

$[Me_2Co(DpnH)]$, mmol	time, s	methane yield, μmol	$[\Delta CH_4]$, μmol	$[C_2H_6]$, μmol	$[C_2H_6]/[\Delta CH_4]$
0.120	579	3.98 (1.27)[b]	2.71	3.32	1.23
0.090	434	2.97 (0.965)[b]	2.01	2.52	1.25
0.060	290	2.04 (0.627)[b]	1.41	1.67	1.18
0.030	145	1.01 (0.334)[b]	0.68	0.85	1.25

[a] In acetonitrile solution containing 1.0 M $CHCl_3$ and 0.1 M TEAP at 25 °C and 2.0 mA. [b] In the absence of $CHCl_3$.

The initial concentration of $Me_2Co(DpnH)$ was also varied, while maintaining the same current level and chloroform concentration. The background reaction was carried out under identical conditions, except in the absence of the chloroform trap. The methane produced in the reaction with chloroform is tabulated as ΔCH_4 in Table V, after correction for the background. The constancy of the ratio of $C_2H_6/\Delta CH_4$ in the last column demonstrates that the relative rate of ethane formation during electrooxidation does not depend on the concentration of $Me_2Co(DpnH)$.[14]

B. Distinction between Methyl Radical and $Me_2Co(DpnH)^+$ as the Source of Methane or Ethane. The trapping of the cleaved methyl ligand as methane and the coupling to ethane are both indicative of a methyl radical as the active precursor. However, it is also conceivable that the dimethylcobalt(IV) cation can react directly with the chemical traps or with itself to yield the same products. The distinction between these two radical species as the active precursor was examined in the following series of studies involving (1) halogen selectivity and (2) ionic strength effects.

1. The determination of the CH_3Cl/CH_3Br selectivity in the anodic oxidation of $Me_2Co(DpnH)$ was carried out in the presence of a mixture of carbon tetrachloride and benzyl bromide as the

(12) Limiting currents were obtained by stepping the voltage to values 80 mV more anodic than E_p and recording the resultant current profile.

(13) At high trap concentrations, the graphs in Figure 4 are observed to be curved. This curvature is accounted for in the detailed analysis of the steady state equations in Scheme III and Figure 8 in the discussion.

(14) The relative rate of ethane formation to the total methane produced is also independent of the $Me_2Co(DpnH)$ concentration.

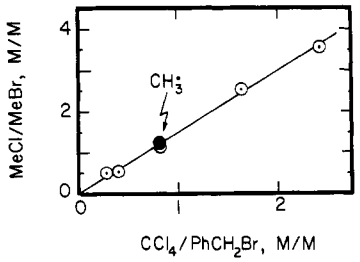

Figure 5. The relative rates of formation of MeCl and MeBr during the electrooxidation of 1.0×10^{-2} M $Me_2Co(DpnH)$ at 2 mA in the presence of various ratios of $CCl_4/PhCH_2Br$ and carried to 10% completion. Methyl radical selectivity (●) determined from acetyl peroxide photolysis.

chemical traps. As shown in Figure 5, the relative yields of CH_3Cl and CH_3Br are linearly related to the molar ratios of CCl_4 and $PhCH_2Br$, as expected from the simple first-order competition established above. Indeed the linear correlation in Figure 5 passes through the origin, and it represents the working relationship for the inherent selectivity of the active radical precursor. In order to determine whether this selectivity is consistent with that of the methyl radical, an independent source of $CH_3\cdot$ was employed from the photolysis of acetyl peroxide,[15] i.e.,

$$CH_3CO_2\text{–}O_2CCH_3 \xrightarrow{h\nu} 2CH_3\cdot + 2CO_2 \qquad (9)$$

An acetonitrile solution of acetyl peroxide was irradiated with a medium-pressure Hg lamp at 25 °C in the presence of an equimolar mixture of CCl_4 and $PhCH_2Br$, i.e.,[16]

$$CH_3\cdot \xrightarrow{CCl_4} CH_3Cl + Cl_3C\cdot \qquad (10)$$

$$CH_3\cdot \xrightarrow{PhCH_2Br} CH_3Br + PhCH_2\cdot \qquad (11)$$

The relative yields of CH_3Cl and CH_3Br are seen in Figure 5 to fall directly on the line determined for the inherent selectivity of the active radical source in the electrolysis of the $Me_2Co(DpnH)$.

2. Ionic strength effects should serve to distinguish between the coupling of either neutral methyl radicals or charged $Me_2Co(DpnH)^+$ radicals as the source of ethane, if the Brønsted–Bjerrum relationship in eq 12 applies.[17] According to

$$\log (k/k_0) = AZ_aZ_b\mu^{1/2} \qquad (12)$$

their formulation of bimolecular processes, the rate of coupling (k/k_0) varies with the square root of the ionic strength μ of the medium when the ionic charges on the reacting species are Z_a and Z_b. [The Brønsted constant A, which is a function of the temperature and the dielectric constant of the solvent, is 1.54 for acetonitrile at 25 °C.[18]] In order to evaluate the effects of ionic strength on ethane formation, the ethane yield was measured relative to that of methane, the rate of which is independent of μ (since $Z_a = 0$ for a chloroform trap). Accordingly, a mixture $Me_2Co(DpnH)$ and chloroform was treated with tris(bipyridine)iron(III) in acetonitrile solutions, varying in ionic strength from 1.5×10^{-2} to 1.0 M sodium perchlorate. The ratio of ethane to methane in Figure 6 is strikingly independent of μ. For comparison, the dashed line in Figure 6 gives the expected scope based on eq 12 for the ethane coupling arising from a pair of positively

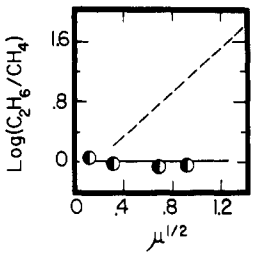

Figure 6. Effect of ionic strength on the relative rates of ethane formation during the oxidation of 2.3×10^{-2} M $Me_2Co(DpnH)$ by 3.0×10^{-2} M $Fe(bpy)_3(ClO_4)_3$ in acetonitrile solution containing 1.0 M $CHCl_3$ as trap and $NaClO_4$ as salt. See text for significance of the dashed line.

charged $Me_2Co(DpnH)^+$ radicals.

Discussion

The dimerization of methyl ligands during the anodic electrolysis of dimethylcobalt(III) macrocycles is reminiscent of other electrochemically induced dimerizations, particularly of organic substrates such as arenes and olefins.[4,5] However, the coupling of methyl ligands differs from the previous mechanistic studies in one important way, namely the primary electron transfer step is not electrochemically reversible. Thus the usual electrochemical methods for the determination of reaction mechanisms which assume a reversible electron-transfer step are not applicable,[8] and alternative approaches which are not restricted by this assumption are required. The clean anodic cleavage of dimethylcobalt(III) macrocycles offers an excellent opportunity to consider this type of electrochemical problem in some detail. In the following discussion, we focus our attention on two principal mechanistic facets of the chemical and electrochemical oxidation of the dimethylcobalt(III) macrocycles, namely (1) the nature of the primary step, and (2) the fast reactions subsequent to the electron-transfer process in which the methyl ligand is oxidatively dimerized. We wish to show how the well-behaved characteristics of the primary electron-transfer process with dimethylcobalt(III) macrocycles allow a detailed mechanistic analysis of ethane formation to be made. By way of contrast, the mechanism of the formation of alkyl dimers in the well-known Kolbe oxidation of carboxylic acids is still a matter of active research.[20]

I. Kinetics and Mechanism of the Electron-Transfer Process. The careful analysis of the shape of the CV wave and the sweep rate dependence of the peak potential (as described in detail in the Experimental Section) demonstrates that the primary anodic processes for the dimethylcobalt(III) macrocycles in Figure 1 and Table I are not electrochemically reversible. [For a discussion of the theory of electrochemical irreversibility as it applies to the kinetics of the electrode process and the analysis of the CV wave as originally developed by Delahay, see Nicholson and Shain, Matsuda and Ayabe, as well as Nadjo and Saveant.[8]] In this study it is important to establish that the irreversibility is not due to a specific problem inherent to the electron-transfer process. Accordingly we first wish to show that the electrochemical oxidation proceeds by an outer-sphere electron-transfer mechanism by comparing it directly with the known homogeneous chemical oxidation under conditions of equivalent thermodynamic driving force. Although it is customary to perform this type of comparison in terms of the inherent rate constants for electron transfer measured at the standard reduction potentials E^0, such a procedure cannot be carried out in this system. An alternative approach must be developed owing to the unavailability of E^0 for the alkylcobalt(III)–alkylcobalt(IV) couple arising from the instability of the oxidized form. We begin by noting that for a totally irreversible electrochemical process, the potential dependence of

(15) (a) Kochi, J. K.; Krusic, P. J. *J. Am. Chem. Soc.* **1969**, *91*, 3940. (b) Pacansky, J.; Gardini, G. P.; Bargon, J. *Ibid.* **1976**, *98*, 2665.

(16) Ingold, K. U. In "Free Radicals"; Kochi, J. K., Ed.; Wiley-Interscience: New York, 1973; Vol. I, p 37ff.

(17) Frost, A. A.; Pearson, R. G. "Kinetics and Mechanism"; J. Wiley and Sons: New York, 1961; 2nd ed, Chapter 7.

(18) (a) Based on ϵ(MeCN) = 37.5[19] and $A = 1.825 \times 10^6(\rho/\epsilon^3T^3)^{1/2}$ where ρ is the density as given by: (b) Moore, W. J. "Physical Chemistry"; Prentice Hall; Englewood Cliffs, N. J., 1972; 4th ed, Chapter 4 and p 356.

(19) Koppel, I. A.; Palm, U. A. In "Advances in Linear Free Energy Relationships"; Chapman, N. B.; Shorter, Y., Eds.; Plenum Press: London, 1972; Chapter 5.

(20) (a) Plyzak, V.; Wendt, H. *Ber. Bunsenges. Phys. Chem.* **1979**, *83*, 481. (b) Tyurin, Y. M.; Smirnova, *Elektrokhimiya* **1979**, *15*, 445. (c) Vijh, A. K.; Conway, B. E. *Chem. Rev.* **1967**, *67*, 623. (d) Gurjar, V. G. *Chem. Ind. Dev.* **1976**, *10*, 15. (e) Eberson, L. In "Organic Electrochemistry"; Baizer, M., Ed.; Dekker: New York, 1969; pp 469. The question of surface films and the uncertainty of free alkyl radicals are still a matter of concern in the mechanism of the Kolbe oxidation.

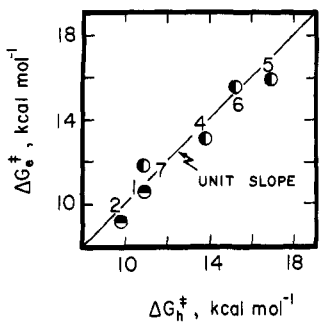

Figure 7. Comparison of the heterogeneous activation free energy $\Delta G_e^{\ddagger}$ and the homogeneous activation free energy $\Delta G_h^{\ddagger}$ from the rate data in Table IV [hexachloroiridate(IV) (◓) and tris(phenanthroline)iron(III) (◐), as oxidants.] The numbers refer to the entries in Table IV. The line is arbitrarily drawn with a slope of unity to emphasize the correlation, as described in the Experimental Section.

the heterogeneous rate constant $k(E)$ for electron transfer is readily calculated (in units of cm s^{-1}) from eq 13,[8b,d] as elaborated in an earlier study,[9]

$$k(E) = 2.18\left[\frac{D\beta\mathcal{F}v}{RT}\right]^{1/2}\exp\left[\frac{\beta\mathcal{F}}{RT}(E - E_p)\right] \quad (13)$$

where D is the diffusion coefficient in cm^2/s, β the transfer coefficient, and v the sweep rate in V/s. The rates of the electrochemical oxidation of the various alkylcobalt(III) macrocycles listed in Table IV were obtained with the aid of eq 13, using values of the applied potential E which correspond to the reversible electrode potentials of the outer-sphere oxidants used in this study, viz., 0.43 V for hexachloroiridate(IV), 0.98 V for tris(phenanthroline)iron(III), 0.98 V for tris(bipyridine)iron(III), and 1.18 V vs. NaCl-SCE for tris(5-nitrophenanthroline)iron(III) in acetonitrile solutions.[21]

In order to compare the rates of the heterogeneous electrode process and the homogeneous chemical oxidation, the rate constants in Table IV were converted to the free energies of activation given by:

$$\Delta G^{\ddagger} = -RT \ln k/Z \quad (14)$$

where the collision frequencies Z for the heterogeneous (Z_e) and the homogeneous (Z_h) rate processes were taken as 3.5×10^3 cm s^{-1} and 3.0×10^{10} M^{-1} s^{-1}, respectively.[22] The correlation between the rate processes for the heterogeneous and homogeneous oxidations designated as $\Delta G_e^{\ddagger}$ and $\Delta G_h^{\ddagger}$, respectively, is illustrated in Figure 7.[23] The fit of the points to the dashed line, arbitrarily drawn with a slope of unity and passing through the origin, underscores the essential outer-sphere mechanism for the electron-transfer oxidation of these organocobalt(III) macrocycles. Indeed such a linear correlation derives directly from Marcus theory, as described separately at the end of this paper (vide infra).

At this juncture, we wish to comment briefly on the applicability of eq 13 for the evaluation of the heterogeneous rate constants $k(E)$ for electron transfer from the alkylcobalt(III) macrocycles examined in this study, since it was originally developed for the limiting case of total electrochemical irreversibility, i.e., rate-limiting electron transfer.[9] However, the magnitudes of the transfer coefficients β for the alkylcobalt(III) macrocycles listed in Table I are larger than 0.5, which raises the possibility of *partial* electrochemical reversibility, i.e., mixed kinetic control.[8c] Since this uncertainty in the electrode kinetics could affect the significance of the correlation in Figure 7, we have carried out a rigorous analysis of the error in eq 13 introduced by mixed kinetic control. For the degree of electrochemical irreversibility as measured by the apparent transfer coefficients in Table I, we indeed find the error in the application of eq 13 to be less than 0.2 kcal mol^{-1}. [See Figure 11 and the analysis in the Experimental Section.] Such limited magnitudes of the error are easily encompassed within the scatter of points from the linear correlation in Figure 7.

II. Mechanism of Ethane Formation. The deuterium-labeling studies have established that ethane arises from an intermolecular process in which methyl ligands from two separate organocobalt species are randomly dimerized. This result, coupled with the coulometric data in Table II which indicates a net one-electron oxidation, suggests that ethane may be produced in an associative pathway such as that in Scheme I involving an organocobalt(IV) intermediate. (Indeed Scheme I is reminiscent of a generally discussed electrochemical mechanism involving the coupling of a reversibly formed radical with its parent.[4,5] For clarity, the macrocyclic ligand is omitted in this and in the following schemes.)

Scheme I

$$Me_2Co^{III} \xrightarrow{k} Me_2Co^{IV} + e^- \quad (15)$$

$$Me_2Co^{IV} + Me_2Co^{III} \overset{K}{\rightleftharpoons} [Me_2Co^{IV}Me_2Co^{III}] \quad (16)$$

$$[Me_2Co^{IV}Me_2Co^{III}] \rightarrow MeCo^{III} + MeCo^{II} + Me_2 \quad (17)$$

$$MeCo^{II} \xrightarrow{\text{fast}} MeCo^{III} + e^- \quad (18)$$

In this mechanism, the methyl ligand is transferred in eq 17 from one cobalt to another within the mixed valence complex. Indeed, examples of such alkyl transfers in binuclear metal complexes are well-known in the organometallic literature.[26] The second electron transfer in eq 18 is expected to occur readily at the applied potential of 0.5 V, since the cyclic voltammogram of MeCo(DpnH)$^+$ exhibits a cathodic wave at −1.05 V vs. SCE. An alternative mechanism involving a two-electron oxidation followed by synproportionation is shown in Scheme II. Although these possibilities are mechanistically distinct, they both predict second-order kinetics, which is first order in the unoxidized dimethylcobalt(III) macrocycle. However, when the rate of formation of ethane is measured relative to the reaction with chloroform, stoichiometrically depicted as,

Scheme II

$$Me_2Co^{III} \rightarrow Me_2Co^{V} + 2e^- \quad (19)$$

$$Me_2Co^{V} + Me_2Co^{III} \rightarrow 2MeCo^{III} + Me_2 \quad (20)$$

$$Me_2Co(DpnH)^+ + CHCl_3 \rightarrow MeCo(DpnH)^+ + MeH, \text{ etc.} \quad (21)$$

it showed no measurable dependence on the concentration of Me$_2$Co(DpnH).[27] The kinetics by competition are thus sufficient

(21) Wong, C. L.; Kochi, J. K. *J. Am. Chem. Soc.* **1979**, *101*, 5593.

(22) The collision frequencies for the heterogeneous and homogeneous electron transfers were calculated by using the following expressions: $Z_e = (RT/2\pi M)^{1/2}$ and $Z_h = 10^3 N(8\pi RT/\bar{M})^{1/2}r^2$, where N is Avogadro's number, M is the molecular weight, $\bar{M}$ is the reduced molecular weight of the reactant pair, and r is the distance separating the reactants. An average mass of 350 and a distance of 7×10^{-8} cm were used to obtain $Z_e = 3.5 \times 10^3$ cm s^{-1} and $Z_h = 3 \times 10^{10}$ M^{-1} s^{-1}. See ref 9, 18b, and: Savéant, J. M., Tessier, D. *J. Phys. Chem.* **1977**, *81*, 2192.

(23) The values of $\Delta G^{\ddagger}$ for hexachloroiridate(IV) have been corrected by 3.3 kcal mol^{-1} for the reorganization energy,[24] but that for the iron(III) oxidant was assumed to be nil.[25]

(24) See: Pelizzetti, E.; Mentasti, E.; Praumauro, E. *J. Chem. Soc., Perkin Trans. 2* **1978**, 620. Hurwitz, P.; Kustin, K. *Trans. Faraday Soc.* **1966**, *62*, 427.

(25) See: Brown, G. M.; Sutin, N. *J. Am. Chem. Soc.* **1979**, *101*, 883.

(26) Kochi, J. K. "Organometallic Mechanisms and Catalysis"; Academic Press: New York, 1978; Chapter 18 and references therein. (b) Norton, J. R. *Acc. Chem. Res.* **1979**, *12*, 139. (c) Bergman, R. G. *Ibid.* **1980**, *13*, 113. (d) Tsou, T. T.; Kochi, J. K. *J. Am. Chem. Soc.* **1979**, *101*, 883.

(27) When using relative rate data, it is important to establish that the monitoring reaction does not occur after the product-determining step. For the mechanism in Scheme I, this could occur if the monomethylcobalt(III) species reacted with $CHCl_3$ to yield methane. Such a possibility is ruled out by the observation that $CHCl_3$ affects neither the total yield of the cleaved methyl groups nor the yield of MeCo(DpnH)$^+$. For additional examples of the use of competition experiments in electrochemistry, see: Saveant, J. M. *Acc. Chem. Res.* **1980**, *13*, 323.

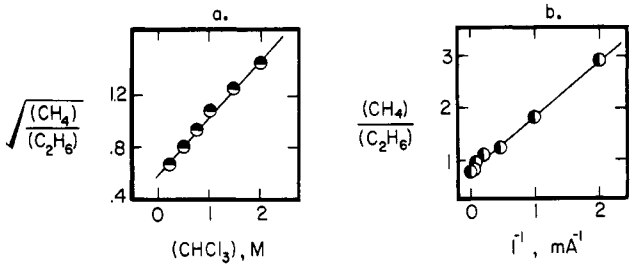

Figure 8. The verification of the steady state predictions based on the methyl radical as the reactive species in ethane and methane formation during the anodic oxidation of 10^{-2} M $Me_2Co(DpnH)$ in acetonitrile carried to 10% completion: (a) at 2 mA in the presence of various amounts of chloroform and (b) in 1 M $CHCl_3$ at various applied currents.

to rule out the mechanisms in Schemes I and II.

Taken together these observations indicate that a pair of dimethylcobalt(IV) cations are the precursors in the production of ethane. Such a mechanism may derive from homolytic scission, e.g.,

$$Me_2Co(DpnH)^+ \rightarrow MeCo(DpnH)^+ + Me\cdot \qquad (22)$$

followed by the rapid coupling of the methyl radicals. Furthermore, such methyl radicals are known to be efficiently trapped by chloroform, carbon tetrachloride, and benzyl bromide,[16] in accord with the observations in Figure 4. This argument is not compelling, however, since it is also possible for the paramagnetic dimethylcobalt(IV) species to react directly with these added reagents. Similar reactions have recently been shown for paramagnetic organonickel(III) and organoiron(III) species.[28]

The distinction between methyl radicals and dimethylcobalt(IV) cations as the reactive species leading to ethane can be made on the basis of two different kinds of studies. First, the competitive selectivity of the active methyl species toward halogen-atom transfer from carbon tetrachloride and benzyl bromide was shown in Figure 5 to be identical with that of the methyl radical generated independently from the acetyl peroxide photolysis in eq 9.[29] Secondly, the relative rate of ethane production during the oxidation of $Me_2Co(DpnH)$ shows no dependence on the ionic strength of the medium—a fact which is inconsistent with a bimolecular reaction of two dimethylcobalt(IV) cations according to the Brønsted–Bjerrum formulation in eq 12.

The mechanism presented in Scheme III accords with all the

Scheme III

$$Me_2Co^{III} \xrightarrow{k_1} Me_2Co^{IV} + e^- \qquad (23)$$

$$Me_2Co^{IV} \xrightarrow{k_2} MeCo^{III} + Me\cdot \qquad (24)$$

$$Me\cdot + SH \xrightarrow{k_3} MeH + S\cdot \qquad (25)$$

$$2Me\cdot \xrightarrow{k_4} Me_2 \qquad (26)$$

$$Me\cdot + XY \xrightarrow{k_5} MeX + Y\cdot \qquad (27)$$

experimental data extant on the oxidative cleavage of dimethylcobalt(III) macrocycles. The trapping reactions with XY = chloroform, carbon tetrachloride, benzyl bromide, and hexachloroiridate(IV) are included in eq 27. The background reaction with solvent in eq 25 represents a pseudo-first-order process.[30] The mechanism in Scheme III is consistent with the absence of an effect of $Me_2Co(DpnH)$ concentration on the relative yields of ethane and methane. Moreover, there are two additional ex-

(28) Compare: Tsou, T. T.; Kochi, J. K. *J. Am. Chem. Soc.* **1978**, *100*, 1634.

(29) The use of selectivity as a criterion for the identification of reactive intermediates depends on the use of substrates with different polar properties, see: Russell, G. A. in ref 16, Chapter 7.

(30) Abstraction of hydrogen from the macrocyclic ligand has also been noted during the photolysis of $MeCo(TIM)^{2+}$ by Mok, C. Y.; Endicott, J. F. *J. Am. Chem. Soc.* **1978**, *100*, 123.

Table VI. The Comparative Effectiveness of Various Chemical Trapping Agents in the Anodic Oxidation of $Me_2Co(DpnH)$

chemical trap	slope,[a] M^{-1}	k_5,[b] 10^{-3} M^{-1} s^{-1}	slope/k_5, 10^5 s^{-1}
$CHCl_3$	0.43	4.47	9.6
CCl_4	0.13	1.30	10
$PhCH_2Br$	0.24	2.00	12

[a] Compare Figure 8a, determined as $d([CH_3X]/[C_2H_6])^{1/2}/d[trap]$. [b] Data from ref 33.

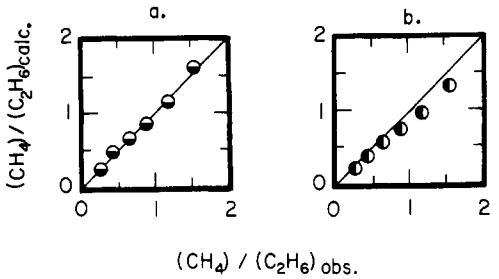

Figure 9. Agreement of the calculated and observed product ratios based on the kinetics in Scheme III utilizing Saveant's method (left) and Feldberg's procedure (right). The points correspond to the various concentrations of chloroform in Figure 8a. [Note the abscissas are defined differently in Figures 8a and 9.] See text for the discussion of the rate constants and the Experimental Section for the calculations. The lines are arbitrarily drawn with a slope of unity to emphasize the fit.

perimental parameters which may be used to verify this scheme, namely, the applied current and the concentration of the chloroform trap. The steady state analysis of the mechanism in Scheme III yields the relationship in eq 28, where V represents

$$\left(\frac{[CH_4]}{[C_2H_6]}\right)^{1/2} = \left[\frac{V}{k_4k_1}\right]^{1/2}(k_3 + k_5[CHCl_3]) \qquad (28)$$

the effective volume of the solution in which ethane formation occurs, as elaborated in the Experimental Section. According to Scheme III, the ratio of methane to ethane should be inversely proportional to the applied current, which is directly related to the rate constant for electron transfer k_1. Furthermore, at a constant current, the square root of this ratio should be proportional to the chloroform concentration. Both of these predictions are borne out by the experimental data plotted in Figures 8a and 8b. Equation 28 also predicts that the slope of Figure 8a should be directly proportional to k_5, the rate constant for the reaction between the methyl radical and the trap. The data in column 4 of Table VI clearly bear out this prediction. The mechanism in Scheme III is thus consistent with the dependence of the relative yield of ethane on the four experimental parameters, namely: (1) the concentration of the dimethylcobalt(III) macrocycle, (2) the applied current, (3) the concentration of the chemical traps, and (4) the relative reactivities of the different chemical trapping agents.

According to Scheme III, the high yields of ethane arise from the instability of the alkylcobalt(IV) cationic intermediate and the attendant high flux of methyl radicals which can be generated. Indeed the observed product ratio, $(CH_4)/(C_2H_6)$, in Figure 8a may be used to evaluate the lifetime of the dimethylcobalt(IV) cation, by utilizing two generalized methods developed for electrochemical kinetics.[31,32] In Saveant's reaction layer model,[32] the diffusion layer is divided into two zones: an inner layer analyzed by steady state methods and an outer layer in which the concentrations of the unstable intermediates are assumed to be zero. The agreement between the calculated and the observed product ratios is shown in Figure 9a at several concentrations of chloroform. The calculations (described in the Experimental

(31) Feldberg, S. W. *Electroanal. Chem.* **1969**, *3*, 200.

(32) Amatore, C.; Saveant, J. M., to be published (private communication).

Section) were carried out with known values[33] of the rate constants $k_4 = 5 \times 10^9$ M^{-1} s^{-1} and $k_5 = 4.47 \times 10^3$ M^{-1} s^{-1}, and then fitting the first-order rate constant k_2 for the decomposition of the dimethylcobalt(IV) cation and the background rate constant k_3 for hydrogen abstraction as 7×10^5 s^{-1} and 1.6×10^3 s^{-1}, respectively. [The measured diffusion coefficient of dimethylcobalt(III) macrocycle is 1.4×10^{-5} cm^2 s^{-1} (see Experimental Section), and that for the methyl radical was taken as 4×10^{-6} cm^2 s^{-1}.[34]] Using the rate constants obtained with the Saveant procedure, we recalculated the product ratio with the use of Feldberg's digital simulation technique,[31] in which the system of differential equations describing the kinetics of the reactions in Scheme III in conjunction with Fick's laws of diffusion are explicitly solved. The results in Figure 9b show that the product ratio is indeed adequately described by values of k_2 and k_3 determined by the two independent methods. We have thus shown that the kinetics in Scheme III afford absolute yields of ethane which are consistent with a highly unstable dimethylcobalt(IV) cation–radical with a lifetime in the order of 10^{-5} s. [For the reliability of this value for the lifetime, see the Experimental Section.]

Summary and Conclusions

Cyclic voltammetry of the *trans*-dimethylcobalt(III) macrocycles, $Me_2Co(DpnH)$ and $Me_2Co(TIM)^+$, shows that the anodic oxidation is due to a chemically irreversible EC electrochemical process. The rates of electron transfer for the heterogeneous electrode process, which correlate in Figure 7 with the rates of the homogeneous oxidations carried out with a series of polypyridineiron(III) and hexachloroiridate(IV) oxidants, underscore the essential outer-sphere mechanism for electron transfer from these organocobalt(III) macrocycles.

The formation of ethane stems from a series of fast reactions which occur subsequent to the electron-transfer process. The rates of the following chemical reactions are observed to be competitive with that of the reverse electron-transfer step as witnessed by the lack of electrochemical reversibility. This limiting kinetic situation is examined in detail, since it is characteristic of irreversible electron-transfer processes. The kinetics of ethane formation can be determined by a competition method in which the monitoring reaction is provided by the interception of the cleaved methyl ligand by hydrogen and halogen atom sources ($CHCl_3$, CCl_4, and $PhCH_2Br$). The rate of ethane formation is determined by the rate of formation of the dimethylcobalt(IV) intermediate (i.e., the rate of oxidation), and it is not otherwise dependent on the dimethylcobalt(III) concentration. The spontaneous homolysis of the transient dimethylcobalt(IV) species to methyl radicals accords with the steady state and the rigorous kinetic analysis of the mechanism in Scheme III, including the dependence on the applied current, and the concentrations of $CHCl_3$ as well as the dimethylcobalt(III) macrocycle.

Experimental Section

Materials. The macrocyclic ligand $DpnH_2$ and the cobalt(III) complexes, $Cl_2Co(DpnH)$, $MeCo(DpnH)(H_2O)ClO_4$, $Br_2Co(TIM)ClO_4$, $(H_2O)_2Co(TIM)(ClO_4)_3$, and $MeCo(DpnH)(H_2O)(ClO_4)_2$, were prepared according to the procedures described in the literature.[35] Since the successful synthesis of the dimethylcobalt(III) complexes was found to be highly dependent on the experimental conditions, they are described separately in detail below. The oxidants, $Fe(phen)_3(ClO_4)_3$, $Fe(bpy)_3(ClO_4)_3$, $Fe(5\text{-Cl-phen})_3(ClO_4)_3$, and $Cu(O_3SCF_3)_2$ were prepared previously.[21,36] $Ag(O_2CCF_3)$ and $Ag(O_3SCF_3)\cdot{}^1/_2C_6H_6$ were prepared in benzene from the treatment of Ag_2O with trifluoroacetic and trifluoromethanesulfonic acids, respectively. $Na_2IrCl_6\cdot 6H_2O$ from Varlacoid Chemical Co. and tetraethylammonium perchlorate and ceric ammonium nitrate from G. F. Smith Chemical Co. were used without purification.

Reagent grade acetonitrile was refluxed over calcium hydride for several hours and then directly distilled. The distillate was redistilled twice from fresh batches of 3:2 mixtures of $KMnO_4$ and anhydrous K_2CO_3. It was then refluxed over CaH_2 again and redistilled from phosphorus pentoxide. Acetonitrile-d_3 was first stirred with freshly activated alumina and then transferred in vacuo.

$Me_2Co(DpnH)$. According to the method of Witman and Weber,[37] 12 g (33 mmol) of $Cl_2Co(DpnH)$ and 14.4 g (65 mmol) of $Ag(CF_3CO_2)$ were combined in 200 mL of reagent grade methanol. The mixture was refluxed for 1 h in the dark to insure the complete precipitation of AgCl. The solution was cooled in an ice bath and then filtered through Celite. The red brown filtrate was placed in a 2-L Erlenmeyer flask and immersed in an ice bath, thereupon 24 g (60 mmol) of NaOH in 15 mL of H_2O was slowly added, after which 15 mL (243 mmol) of purified MeI was added. Subsequently, 4.0 g (105 mmol) of $NaBH_4$ in 15 mL of H_2O was slowly added while the flask was vigorously swirled. After 10 min, masses of orange crystals precipitated. These were collected, washed with several portions of H_2O, air dried, and recrystallized from a mixture of H_2CCl_2 and MeCN: yield, 8.0 g (76%); ϵ_{410} 7.28×10^3 M^{-1} cm^{-1} in MeCN; NMR (pyridine) δ 0.52 (s, 6 H), 2.05 (s, m, 8 H), 2.23 (6 H), 3.62 (t, 4 H). A similar procedure was followed in the preparation of $(CD_3)_2Co(DpnH)$.

$Me_2Co(TIM)BPh_4$.[35a,b] This bright orange-red complex was prepared at 0 °C both under argon and air by the addition of a large excess of $NaBH_4$ to a dilute solution of $(H_2O)_2Co(TIM)ClO_4$ in 4:1 acetone–methanol containing a large excess of MeI. The product was isolated from the bright orange-red solution by the addition of 1 equiv of $NaBPh_4$, followed by concentration of the solution with the use of a rotary evaporator with very gentle heating: yield, 75%. **$Me_2Co(TIM)ClO_4$** was prepared under argon according to the method used for the tetraphenylborate complex, with the exception that an excess of perchlorate was present during reaction. Concentration of the reaction mixture, using very gentle warming, produced a bright orange-red solid which was recrystallized from a mixture of H_2CCl_2 and absolute ethanol: yield, 50%; ϵ_{440} 7.65×10^3 M^{-1} cm^{-1}; NMR (CD_3CN) δ 0.28 (s, 6 H), 2.3 (s, m, 16 H), 3.80 (m, 8 H).

Spectral Titrations. Spectral titrations were performed by adding known quantities of a stock solution of a cobalt(III) complex to volumetric flasks containing a known aliquot of the oxidant. Reaction was complete upon mixing, after which the contents were diluted to volume. The absorption spectrum was recorded on a Cary 14 spectrophotometer. The results were independent of the order of mixing, and the reagent in excess. In a typical example, 0.5 mL of an 8.6×10^{-3} M solution of $Fe(phen)_3(ClO_4)_3$ was placed in a 5-mL volumetric flask which had been thoroughly flushed with argon. Then 0.2 mL of a 7.6×10^{-3} M solution of $Me_2Co(DpnH)$ was added. After the reaction was complete, the solution was diluted to volume and its absorption spectrum recorded. The absorbance at 510 nm indicated an iron(II) concentration of 2.7×10^{-4} M. This value corresponded to a cobalt(III)/iron(III) stoichiometry of 1.09. A plot of the absorbance against the ratio of iron(III) to cobalt(III) yielded a stoichiometry of 1.05.

Analysis of the Volatile Products. The following procedure is representative: 0.070 g (0.085 mmol) of $Fe(bpy)_3(ClO_4)_3$ was placed into a 25-mL round-bottom flask and sealed with an undyed serum stopper. The flask was flushed with either argon or oxygen, after which 3 mL of argon- or oxygen-saturated MeCN was added. Following this, 2 mL of a 0.02 M solution of $Me_2Co(DpnH)$ was added to the rapidly stirred iron(III) solution. Ethylene (0.5 mL) was added as an internal standard and the flask was equilibrated at 0 °C. Methane and ethane were analyzed at 55 °C on a Varian aerograph model 3700 gas chromatograph equipped with a 4-ft Porapak Q column and automatic integrator. The reaction carried out under argon produced 0.001 mmol of CH_4 and 0.018 mmol of C_2H_6, corresponding to 95% recovery of 1 equiv of methyl groups. Similar procedures were utilized with the other oxidants. Methyl chloride produced in the reactions of $Na_2IrCl_6\cdot 6H_2O$ was analyzed at 70 °C, using a 10-ft column of dibutyl tetrachlorophthalate on chromosorb P. The results are presented in columns 4–7 of Table VII.

NMR Analyses of Reaction Products. In a typical experiment, 0.0276 g (0.084 mmol) of $Me_2Co(DpnH)$ and 0.0179 g (0.02 mmol) of $Fe(phen)_3(ClO_4)_3$ were weighed into an NMR tube, which was then sealed with a serum stopper and thoroughly flushed with argon. Thereupon, 0.5 mL of CD_3CN was added and the tube vigorously shaken. Upon completion of reaction, the tube was flushed with argon to remove C_2H_6 and

(33) Macken, K. V.; Sidebottom, H. W. *Int. J. Chem. Kinet.* **1979**, *11*, 511. See also Edwards, F. G.; Mayo, F. R. *J. Am. Chem. Soc.* **1950**, *72*, 1265.

(34) Since the diffusion coefficient of the methyl radical is unmeasured, the value was taken for that of similar alkyl radicals reported by: Burkhart, R. D.; Wong, R. J. *J. Am. Chem. Soc.* **1973**, *95*, 7203, and references therein.

(35) (a) Witman, M. W.; Weber, J. H. *Inorg. Chim. Acta*, **1977**, *23*, 263. (b) Farmery, K.; Busch, D. H. *Inorg. Chem.* **1972**, *11*, 2901. (c) Jackels, S. C.; Farmery, K.; Barefield, E. K.; Rose, N. J.; Busch, D. H., *Inorg. Chem.* **1972**, *11*, 2893.

(36) Ford-Smith, M. H.; Sutin, N. *J. Am. Chem. Soc.* **1961**, *83*, 1830. (b) Dwyer, F. P.; McKenzie, H. A. J. *Proc. R. Soc. S. Wales* **1947**, *81*, 93. (c) Jenkins, C. L.; Kochi, J. K. *J. Am. Chem. Soc.* **1972**, *94*, 843. (d) See also ref 16.

(37) Witman, M. W.; Weber, J. H. *Synth. React. Inorg. Met.-Org. Chem.* **1977**, *7*, 143.

Table VII. Products in the Oxidative Cleavage of *trans*-Dialkylcobalt(III) Macrocyclic Complexes

$[Me_2Co(DpnH)]$ or $[Me_2Co(TIM)ClO_4]$, 10^2 mmol	stoichiometry[a] oxidant, 10 mmol	Co(III)/ oxidant	concn of products CH_4, 10^4 mmol	C_2H_6, 10^3 mmol	MeCl, 10^2 mmol	$Me_2Co(III)$[b]/ oxidant
$Me_2Co(DpnH)$						
3.3	$Fe(phen)_3(ClO_4)_3$, 1.1	1.03 (Ar)	5	16		1.0 (Ar)
		1.02 (O_2)[c]	<1	2.1		1.0 (O_2)
3.3	$Fe(bpy)_3(ClO_4)_3$, 0.91	0.94 (Ar)	5	16		1.0 (Ar)
		1.04 (O_2)[c]	<1	1.6		1.0 (O_2)
2.5	$Fe(5\text{-Cl-phen})_3(ClO_4)_3$, 0.41	0.99 (Ar)	50	9.0		1.0 (Ar)
2.2	$Na_2IrCl_6 \cdot 6H_2O$, 0.80	0.51 (Ar)	1	0.1	2.0	0.5 (Ar)
		0.82 (O_2)[c]	<1	<0.1	1.8	0.8 (O_2)
3.6	$(PPN)_2IrCl_6$, 0.69	0.57 (Ar)	7	0.6	3.2	0.5 (Ar)
4.0	$Cu(OTf)_2$, 1.5	1.05 (Ar)	<1	19		1.0 (Ar)
		(O_2)[c]	<1	5.3		1.0 (O_2)
4.0	Ag(OTf), 1.8	0.99 (Ar)	5	20		1.0 (Ar)
			<1	7.5		
2.4	$Fe(phen)_2(CN)_2$, 0.41	1.01 (Ar)	19	11		1.0 (Ar)
3.8	$(NH_4)_2Ce(NO_3)_6$, 0.80	1.03 (Ar)	25	17		1.0 (Ar)
3.8	$MeCo(DMG)_2py^+$, 0.37	0.96 (Ar)	10	18		1.0 (Ar)
$Me_2Co(TIM)ClO_4$						
3.0	$Fe(phen)_3(ClO_4)_3$, 1.8	0.86 (Ar)	5	9.1		0.78 (Ar)
		0.90 (O_2)[c]	<1	<0.1		
3.0	$Cu(OTf)_2$, 2.4	0.95 (Ar)	3	3		0.67 (Ar)
		(O_2)[c]	<1	<0.1		
2.0	$Na_2IrCl_6 \cdot H_2O$, 0.75	0.52 (Ar)	2	0.1	2.0	0.55 (Ar)
		0.81 (O_2)[c]	<1	<0.1	1.4	0.74 (O_2)

[a] Average values obtained from spectral titrations and NMR analyses. [b] Determined by NMR analyses; oxidant is the limiting reagent. [c] Reactions carried out under 1 atm of O_2.

CH_4. The NMR spectrum compared favorably with that of an authentic sample of $MeCo(DpnH)(H_2O)ClO_4$: δ 0.82 (s, 3 H), 2.32 (s, m, 8 H), 2.33 (s, 6 H), 3.73 (m, 4 H). After the addition of 0.12 mmol of diphenylmethane, the integration of the NMR spectrum indicated the production of 0.023 mmol of $MeCo(DpnH)(MeCN)ClO_4$ which corresponded to a cobalt(III):iron(III) stoichiometry of 1.15. Analogous results were obtained under oxygen, as included in column 7 of Table VII.

Deuterium-Labeling Experiments. Ethane Analysis. $(CH_3)_2Co(DpnH)$ and $(CD_3)_2Co(DpnH)$ were combined in acetonitrile solutions with the use of the following molar ratios: 1:0, 1:1, 7:3, 3:7, and 0:1. An aliquot of 2.0 mL of each mixture was added to a rapidly stirred solution containing an excess of either $Fe(phen)_3(ClO_4)_3$ or $Cu(CF_3SO_3)_2$. The isotopic composition of the ethane produced was determined by using a Hewlett-Packard HP-5992A GC-MS which was equipped with a 4-ft Porapak Q column. The cracking patterns for d_0 and d_6 ethane were obtained under the experimental conditions from authentic samples. The pattern for CD_3CH_3 was calculated from literature values.[11]

Electrochemical Measurements. Electrochemistry was performed on a Princeton Applied Research Model 173 potentiostat which allows the electrolysis to be performed under conditions of constant potential or constant current. The potentiostat was equipped with a Model 176 current-to-voltage converter which provided a feedback compensation for ohmic drop between the working and reference electrodes. The voltage follower amplifier (Model 178) was mounted external to the potentiostat with a minimum length of high-impedance connection to the reference electrode. This arrangement insured low noise pickup. Cyclic voltammograms were recorded on a Houston series 2000 *X–Y* recorder. The electrochemical cell was constructed according to the design of Van Duyne and Reilley.[38] The distance between the platinum working electrode and the tip of the salt bridge was 1 mm to insure a minimum ohmic drop. Coulometry was carried out with the use of a three-compartment cell of conventional design with a platinum gauze electrode. Complete electrolysis of 0.1 mmol of $Me_2Co(DpnH)$ generally required 5–10 min, and the current was graphically recorded on a Leeds and Northrup Speedomax strip chart recorder.

The diffusion coefficients were obtained from the analysis of the chronoamperometric *i–t* transient according to the relationship: $it^{1/2} = n\mathcal{F}AC(D/\pi)^{1/2}$, as described previously.[9] In all cases, the product $it^{1/2}$ was observed to be constant for periods up to 6 s. The area of the electrode S was calibrated with ferrocene,[5b] in which the diffusion coefficient $D = 2.4 \times 10^{-5}$ cm^2 s^{-1}. For the cobalt(III) complexes, D is evaluated as: $Me_2Co(DpnH)$, 1.5×10^{-5}; $Me_2Co(TIM)^+$, 1.3×10^{-5}; $MeCo(DpnH)^+$, 1.4×10^{-5}; and $EtCo(DpnH)^+$, 1.4×10^{-5} cm^2 s^{-1}.

Electrochemical Reversibility of the Cyclic Voltammetric Waves. The cyclic voltammogram of $Me_2Co(DpnH)$ exhibited a well-defined anodic wave, the peak potential E_p of which is independent of the concentration in the range between 10^{-4} and 10^{-2} M in acetonitrile solutions. In order to evaluate the electrochemical reversibility of the anodic oxidation of dimethylcobalt(III) macrocycles, the following criteria, developed in the foregoing study,[9] was applied. First, the plot of E_p or $E_{p/2}$ against the sweep rate (log v) shown in Figure 10 yields slopes greater than 30 mV per decade, indicating that the electron-transfer step is not reversible.[8]

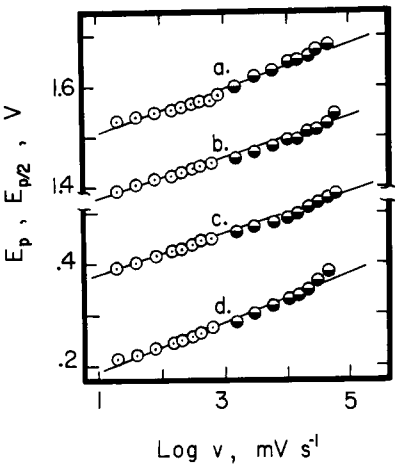

Figure 10. Variation of the anodic peak potentials E_p (⊙) and $E_{p/2}$ (⊖), on the CV sweep rate (log v) at a platinum microelectrode at 25 °C in acetonitrile solutions containing 0.1 M TEAP and (a) 5.43×10^{-3} M $MeCo(DpnH)^+$, (b) 5.40×10^{-3} M $EtCo(DpnH)^+$, (c) 5.6×10^{-3} M $Me_2(DpnH)$, and (d) 8.46×10^{-3} M $Me_2Co(TIM)^+$. [The value of E_p has been shifted by adding 1.857 to log v.]

Table VIII. Consistency in the Transfer Coefficients Determined by Independent Methods[a]

alkylcobalt(III) macrocycle	transfer coefficient E_p vs. log v	$E_p - E_{p/2}$	average
$Me_2Co(DpnH)$	0.77	0.69	0.73 ± 0.05
$Me_2Co(TIM)^+$	0.61	0.55	0.58 ± 0.05
$MeCo(DpnH)^+$	0.62	0.53	0.58 ± 0.05
$EtCo(DpnH)^+$	0.78	0.70	0.74 ± 0.05

[a] See text.

(38) Van Duyne, R. P.; Reilley, C. N. *Anal. Chem.* **1972**, *44*, 142.

Second, the transfer coefficient β obtained from the sweep dependence of the peak potential (see eq 33) is consistent with β determined from the shape of the CV wave (see eq 34). The comparative results are presented in Table VIII, and they indicate that the two independent determinations agree to within 10%. Although these results are consistent with a totally irreversible electron-transfer process, they do not demand it. Thus the observation of slopes in the range between 30 and 60 mV per decade (i.e., $\beta = 1.0$ and 0.5, respectively) does raise the possibility of mixed kinetic control in which the electron transfer process could be described as intermediate between reversible and totally irreversible.[39] Fortunately, it is not necessary to resolve this ambiguity since the analysis in the following section will show that the error in the application of eq 13 or 29 is small, for those electrochemical processes which display a degree of reversibility sufficient to exhibit a transfer coefficient of 0.7.

Quantitative Evaluation of the Error Limits in the CV Method. Recently, we showed how the heterogeneous rate constant for electron transfer could be derived according to eq 29 for a totally irreversible electrode process.[9] However, electrode reversibility is actually a *continuum*, with total irreversibility merely being one limiting extreme.[41] Therefore, it is now necessary to ascertain how eq 29 will perform under actual electrochemical conditions in which electron transfer is only partially reversible. From Scheme III, the potential dependence of the rate constant for forward electron transfer $k(E)$ in eq 30 is given by the general expression:[42]

$$k(E) = k_s \exp\left[\frac{\beta n\mathcal{F}}{RT}(E - E^0)\right] \tag{30}$$

where E is the electrode potential, β is the transfer coefficient for the electrode process, n is the number of electrons transferred in the rate-limiting step, and E^0 is the standard potential which fixes the value of k_s (i.e., $k_s = k_1$ at $E = E^0$). The effectiveness in applying eq 29 to the mechanism in Scheme III was evaluated by the following procedure. Initially, the set of values for the four parameters, k_s, β, k_2, and v, describing the standard electron-transfer rate constant, the transfer coefficient, the homogeneous chemical rate constant, and the CV sweep rate, respectively, were used to calculate a theoretical CV wave according to Saveant's method (vide infra).[8c] In particular, the theoretical CV wave defines the peak potential E_p at which the current maximum will occur. Following this procedure for the determination of E_p, the exact rate of electron transfer at the peak potential is known from eq 30 to be given by:

$$k(E_p) = k_s \exp\left[\frac{\beta n\mathcal{F}}{RT}(E_p - E^0)\right] \tag{31}$$

The result from eq 31 was used to calculate the error in applying eq 29, as an energy difference, i.e.,

$$\text{error} = 2.3RT[\log k(E_p)_{\text{eq 31}} - \log k(E_p)_{\text{eq 29}}] \tag{32}$$

The criteria for experimentally establishing the irreversibility of the electron-transfer step have traditionally been: (1) the slope of the plot of E_p vs. $\log v$, i.e., the sweep rate dependence, and (2) the shape of the CV wave as measured by its width $E_p - E_{p/2}$.[8] Indeed these two observables can be used to obtain quantitative measures of the error in applying eq 29. This is most conveniently carried out by calculating the apparent transfer coefficients β_v and β_w, respectively, as analytical measures of these two experimental parameters with the aid of eq 33 and 34, respectively. Equations 33 and 34 were originally derived by Nicholson and Shain[8b] for a totally irreversible electron-transfer process. In this limit, β_v will be equal to β_w, and both will be equal to the true transfer coefficient β. However, as the electrochemical reversibility increases, values of β_v and β_w will no longer be equal to the true transfer coefficient β. For the purpose of this study, we will only consider the situation corresponding to a fast follow-up chemical reaction in which $k_2 \gg n\mathcal{F}v/RT$. [This chemically irreversible situation is observed experimentally by the absence of a coupled electrochemical wave on the reverse scan of the CV experiment.][8c] Since β_v and β_w, calculated according to eq 33 and 34 for the theoretical CV waves, were observed to be similar for those situations in which $k_2 > n\mathcal{F}v/RT$, we have focussed our attention on only β_w in the subsequent discussion. The rationale behind the use of β_w (or β_v) as a quantitative measure of electrochemical reversibility is best understood by considering the limits of totally reversible and irreversible behavior. For Nernstian charge transfer, the standard electrochemical theory predicts the CV wave to be quite sharp. Indeed the situation with $E_p - E_{p/2} < 1.857RT$ has been described as being superreversible.[43] As the electrochemical process becomes less reversible the wave will broaden—eventually reaching the limit predicted by eq 34 with $\beta_w = \beta$.[44] Figure 11a shows the variation in the error in applying eq 29 with the apparent transfer coefficient β_w calculated at various values of k_s between 10^2 and 10^{-6} cm s^{-1} at a constant ratio of $k_2/(n\mathcal{F}v/RT) = 100$. Thus, by the time the apparent transfer coefficient β_w has dropped to a value of 0.7 or less, the error defined by eq 32 has dropped to 0.2 kcal mol^{-1} or less. In order to insure that this limit is not an artifact of the actual transfer coefficient used in the calculation, the analysis was repeated with $\beta = 0.3$ and 0.7 (see Figure 11a). Finally, it could also be shown that this conclusion was not dependent on the magnitude of the rate constant k_2 of the follow-up chemical reaction. Thus while holding k_s and v constant at 1.0 cm s^{-1} and 259 mV s^{-1}, respectively, the chemical rate constant k_2 in Figure 11b was varied incrementally over the limits of 10 to 10^{20} s^{-1}, using three values of the transfer coefficient $\beta = 0.3$, 0.5, and 0.7. It is important to emphasize that in no case was the error >0.2 kcal mol^{-1} when $\beta \leq 0.7$. In other

$$\beta_v = \left[\frac{2.3RT}{2n\mathcal{F}}\right]\left[\frac{dE_p}{d \log v}\right]^{-1} \tag{33}$$

$$\beta_w = \left[\frac{1.857RT}{n\mathcal{F}}\right][E_p - E_{p/2}]^{-1} \tag{34}$$

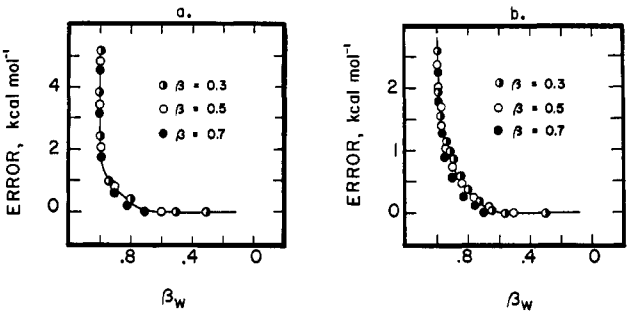

Figure 11. The relationship between the error in log $k(E_p)$ evaluated by eq 32. Left figure: $D = 1.0 \times 10^{-5}$ cm^2 s^{-1}, $v = 259$ mV s^{-1}, $k_2/(n\mathcal{F}v/RT) = 100$, $10^2 > k_s > 10^{-6}$ cm s^{-1}, $\beta = 0.3$, 0.5, and 0.7. Right figure: $D = 1.0 \times 10^{-5}$ cm^2 s^{-1}, $v = 259$ mV s^{-1}, $k_s = 1.0$ cm s^{-1}, $10 < k_2 < 10^{20}$ s^{-1}, $\beta = 0.3$, 0.5, and 0.7.

Table IX. Definition of Dimensionless Variables for the Computation of CV Waves

laboratory parameter	dimensionless parameter	description	defining equation
k_s	Λ	standard rate constant for electron transfer	$\Lambda = k_s(Dn\mathcal{F}v/RT)^{-1/2}$
k	λ	first-order chemical rate constant	$\lambda = RTk/n\mathcal{F}v$
E	ξ	applied potential	$\xi = -(n\mathcal{F}/RT)(E - E^0)$
i	ψ	current	$\psi = i(n\mathcal{F}SC^0)^{-1} \times (Dn\mathcal{F}v/RT)^{1/2}$
α, β	no change	transfer coefficients	$\beta = 1 - \alpha$

[a] D is the diffusion coefficient (cm^2 s^{-1}), v is the sweep rate (V s^{-1}), S is the area of the electrode (cm^2), and C^0 is the initial molar concentration of the electroactive species A, according to reference 8c.

(39) Slopes in this range have been theoretically predicted for mixed kinetic control by the charge-transfer step and the follow-up chemical reactions (see Figures 5 and 9 in ref 8c), and they have been observed in the hydrodimerization of benzaldehyde.[40] Alternatively, slopes in this same range are predicted for the case of pure kinetic control by the charge-transfer step for values of the transfer coefficient greater than 0.5.[8c]

(40) Ammar, F.; Nadjo, L.; Saveant, J. M. *J. Electroanal. Chem.* **1973**, *48*, 146.

(41) Klingler, R. J.; Kochi, J. K. *J. Phys. Chem.*, in press.

(42) Bauer, H. H. *J. Electroanal. Chem.* **1968**, *16*, 419.

(43) Evans, D. H. *J. Phys. Chem.* **1972**, *76*, 1160.

(44) These conclusions result directly from eq 33 and 34 and the known response of the limiting cases of a totally reversible and irreversible electrochemical wave.[8]

words, by the time the CV wave shows even small broadening effects, the error in applying eq 29 is quite small.

Calculation of Current–Potential Waves. Theoretical i–E curves for linear sweep (and cyclic) voltammetry for charge transfer followed by an irreversible first-order chemical reaction have been developed by several workers.[8,45] Owing to its generality, we utilized Saveant's method,[8c] in which the input rate constants k_s and k are converted, for ease in computation, to dimensionless variables according to the definitions in Table IX. The resultant current values i_p and peak potentials E_p are consequently also obtained as the unitless parameters ψ and ξ_p, respectively, as defined in Table IX. The current ψ is expressed as a function of the applied potential ξ, and obtained from the solution of the convolution integral in eq 35, in which the input parameters are the electron-

$$\psi\Lambda^{-1}\exp(-\alpha\xi) = 1 - \pi^{-1/2}\int_{-u}^{\xi}\{1 + \exp(-\xi)\exp[-\lambda(\xi-\eta)]\}(\xi-\eta)^{-1/2}\psi\,d\eta \quad (35)$$

transfer rate constant Λ and the chemical rate constant λ in addition to the transfer coefficient β or α. The integration was carried out from an initial potential $-u$, chosen such that the current ψ was equal to 10^{-5}, up to $10^2RT/n\mathcal{F}$ past the peak potential ξ_p. For values of log λ greater than 2, eq 35 was replaced by eq 36.[8c]

$$\psi\Lambda^{-1}\exp(-\alpha\xi) + \psi\lambda^{-1/2}\exp(-\xi) = 1 - \pi^{-1/2}\int_{-u}^{\xi}(\xi-\eta)^{-1/2}\psi\,d\eta \quad (36)$$

A computer program was written to evaluate eq 35 and 36 as a function of Λ, λ, and β and tested by demonstrating that it is capable of reproducing the peak potentials ξ_p and the wave widths, $\xi_p - \xi_{p/2}$, to within 0.2 mV as reported by Saveant (see Tables I–IV in ref 8c). A listing of the FORTRAN program is available upon request.

Electrochemical Oxidation of $Me_2Co(DpnH)$. A solution of 0.12 mmol of $Me_2Co(DpnH)$ and 0.1 M of TEAP in acetonitrile was exhaustively oxidized at 0.70 V vs. NaCl–SCE. The electrolysis required 11.7 C or 1.01 ± 0.05 electrons per cobalt. Analysis of the gaseous products by gas chromatography on a 4-ft Porapak Q column indicated the presence of 0.047 mmol of ethane (78%) and 0.010 mmol of methane (8%). The solvent was removed in vacuo, and the resultant solid residue dissolved in CD_3CN. The ^1H NMR spectrum was identical with that of an authentic sample of $MeCo(DpnH)ClO_4$. The characteristic methyl resonance at δ 0.82 was integrated against a methylene chloride internal standard to yield 0.13 ± 0.01 mmol of $MeCo(DpnH)^+$. The yield of $MeCo(DpnH)^+$ was unaffected by the presence of a $CHCl_3$ trap, since the electrooxidation of a similar solution of $Me_2Co(DpnH)$, but containing 1.0 M $CHCl_3$, also afforded a quantitative yield of $MeCo(DpnH)^+$.

The solvent effect on the electrooxidation of $Me_2Co(DpnH)$ was examined briefly in ethanol. Constant potential oxidation at 0.72 V of 49 μmol of cobalt complex in 12 mL of ethanol containing 0.1 M TBAP yielded 33 μmol of methane and 7.2 μmol of ethane corresponding to an overall 96% accounting of the cleaved methyl group. No methyl ethyl ether (<0.01 μmol) was detected.[46]

Kinetic Measurements. Acetonitrile solutions of cobalt(III) complexes and the oxidants were freshly prepared prior to use. The reactions were carried out under pseudo-first-order conditions with either the cobalt(III) complex or the oxidant in excess. The initial and final spectra were recorded on a Cary 14 spectrophotometer. The reactions were monitored by using a Durrum–Gibson stopped flow spectrophotometer. The rate of disappearance of hexachloroiridate(IV) was followed at 489 nm. The rates of disappearance of $Me_2Co(DpnH)$ and $Me_2Co(TIM)ClO_4$ were followed at 410 and 440 nm, respectively. In these oxidations with iron(III) complexes, the rate of formation of the corresponding iron(II) product was monitored as described previously.[21]

The electrochemical measurements of the relative rates were carried out in acetonitrile solutions of $Me_2Co(DpnH)$ and $CHCl_3$ containing 0.1 M TEAP. The solution was transferred under argon to the electrochemical cell equipped with a rubber serum stopper for the removal of volatile products. Oxidations at a constant current were carried out to 10% completion and calculated according to the relationship: $it = 0.1\mathcal{F}$[mmol of Me_2Co^{III}]. In a typical experiment consisting of 0.12 mmol of $Me_2Co(DpnH)$ and 250 μL of $CHCl_3$ in 12 mL of acetonitrile, the electrolysis was carried out at 25 °C for 580 s at 2 mA. The volatile products, analyzed by gas chromatography on a 4-ft Porapak Q column at 50 °C by using either the method of standard addition or a calibration curve with ethylene as the internal standard yielded 1.86 μmol of CH_4 and 4.37 μmol of C_2H_6.

Ionic strength studies were carried out in a typical experiment in which 0.025 g (0.030 mmol) of $Fe(bpy)_3(ClO_4)_3$ and 0.122 g (1.00 mmol) of anhydrous $NaClO_4$ were placed in a 25-mL Erlenmeyer flask which was equipped with a Teflon-covered stir bar and sealed with a serum stopper. The flask was thoroughly flushed with argon, after which 8 mL of freshly purified acetonitrile was added. Upon dissolution of the iron complex and the electrolyte, 3 mL of purified chloroform was added and the flask was placed in an ice bath. After 10 min, 1 mL of an acetonitrile solution of $Me_2Co(DpnH)$ was added. The CH_4 and C_2H_6 were analyzed by gas chromatography, using the internal standard method.

For the photochemical generation of methyl radicals, a mixture of acetyl peroxide (14.7 μmol), a carbon tetrachloride (2.6 mmol), and benzyl bromide (2.1 mmol), dissolved in 2 mL of acetonitrile and contained in a water-jacketed quartz tube, was irradiated with a medium-pressure Hg lamp at 25 °C. The volatile products were analyzed by gas chromatography by using the internal standard method and yielded CH_4 (0.085 μmol), C_2H_6 (0.135 μmol), CH_3Cl (0.812 μmol), and CH_3Br (0.664 μmol).

Steady State Kinetic Analysis of Methane and Ethane Formation. According to Scheme III, the ratio of methane to ethane is determined from eq 25–27 as:

$$[CH_4]/[C_2H_6] = (k_3 + k_5[CHCl_3])/k_4[CH_3\cdot] \quad (37)$$

The methyl radical concentration in eq 37 is obtained from the steady state assumption as follows. The rate of electron transfer in eq 23 of Scheme III is related to the current according to eq 38. Since the total

$$k_1 = i/n\mathcal{F} \quad (38)$$

irreversibility of the CV wave indicates that the chemical reaction is complete within a short distance of the electrode surface, an approximate kinetic model assumes that the formation of Me_2Co^{IV} occurs at a rate (in units of mol s^{-1}) given by eq 38 over an effective volume of solution V. The steady state equations for the two transients are then given as:

$$d[Me_2Co^{IV}]/dt = k_1/V - k_2[Me_2Co^{IV}] \quad (39)$$

and

$$d[CH_3\cdot]/dt = k_2[Me_2Co^{IV}] - k_3[CH_3\cdot] - 2k_4[CH_3\cdot]^2 - k_5[CHCl_3][CH_3\cdot] \quad (40)$$

Equating eq 39 and 40 yields the quadratic expression:

$$2k_4[CH_3\cdot]^2 + (k_3 + k_5[CHCl_3])[CH_3\cdot] = k_1/V \quad (41)$$

In the presence of a chloroform trap at sufficient concentrations to produce methane as the main product, eq 41 reduces to:

$$[CH_3\cdot] = k_1/V(k_3 + k_5[CHCl_3]) \quad (42)$$

Substitution of eq 42 into eq 37 yields the working expression given in eq 28.

Kinetics of the Mechanism in Scheme III. Exact Solution by Numerical Integration. The digital simulation technique of Feldberg was employed to convert a system of partial differential equations into partial finite difference equations.[31] The dimensions of the space–time grid were determined by taking the time interval Δt to be 10% of the lifetime of the methylcobalt(IV) radical. The distance interval Δd was chosen such that the species with the largest diffusion coefficient would only traverse 45% of Δd during the time interval Δt. Decreasing the size of the grid by a factor of two produced only minor changes of less than 0.1% in the calculated results. The sequence of computations was performed according to the digital simulation flow chart in Figure 3 of ref 31. For each time interval Δt, the following computations were performed: First, the concentration of the cobalt(IV) radical in the distance interval adjacent to the electrode was increased according to the current i in eq 43,

$$\Delta[Co^{IV}] = i\Delta t/S\Delta d \quad (43)$$

where S is the area of the electrode. Second, the concentrations of both the cobalt(IV) and the methyl radical were corrected on the basis of planar diffusion according to eq 28 of ref 31. Third, the concentrations of the radical species were changed according to the kinetics of the mechanism in Scheme III for each of the individual distance intervals. Thus, the cobalt(IV) concentration was decreased by the amount given in eq 44, and the change in the methyl radical concentration by eq 45.

$$\Delta[Co^{IV}]/\Delta t = -k_2[Co^{IV}] \quad (44)$$

$$\Delta[CH_3\cdot]/\Delta t = k_2[Co^{IV}] - (k_3 + k_5[XY])[CH_3\cdot] - 2k_4[CH_3\cdot]^2 \quad (45)$$

(45) (a) Reinmuth, W. H. *Anal. Chem.* **1960**, *32*, 1793. (b) Sevcik, A. *Collect. Czech. Chem. Commun.* **1948**, *13*, 349.

(46) In this regard, the decomposition of dimethylcobalt(IV) macrocycles differs in a significant way from that of the monoalkylcobalt(IV) counterparts.[2]

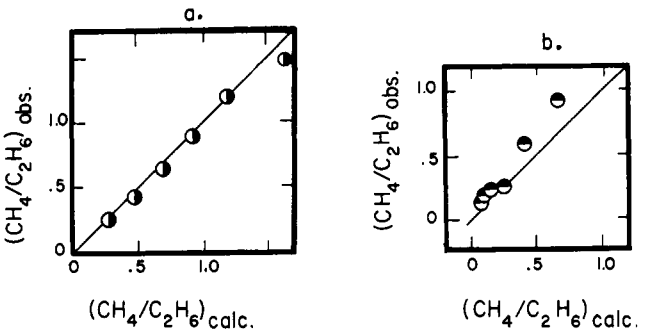

Figure 12. Agreement between the calculated and the observed product ratios with the use of Feldberg's method with $k_2 = 10^5$ s^{-1} and $k_3 = 1.5 \times 10^3$ M^{-1} s^{-1}. Left (a): at various concentrations of chloroform in Figure 8a. Right (b): at various currents in the absence of chloroform. The lines are arbitrarily drawn with a slope of unity.

Finally, the amount of methane and ethane produced in this time interval was added to the running total according to eq 46 and 47, respectively.

$$[CH_4] = [CH_4] + (k_3 + k_5[XY])\Delta t[CH_3\cdot] \quad (46)$$

$$[C_2H_6] = [C_2H_6] + k_4\Delta t[CH_3\cdot]^2 \quad (47)$$

In all cases, a steady state was obtained after approximately 300 cycles of iteration with respect to time. Beyond this point, the total rate of decay of the methylcobalt(IV) radical in solution was equal to the rate of production of this species at the electrode surface. The calculations were carried out for an additional 200 cycles to guarantee convergence. The depth of the reaction layer was calculated to be quite small. Thus 99% of the methylcobalt(IV) radical was decomposed within 6×10^{-5} cm of the electrode surface. This conclusion is consistent with the experimental observation that the product ratio of methane to ethane is independent of the stirring rate. The known values[33] of the rate constants $k_4 = 5 \times 10^9$ M^{-1} s^{-1} and $k_5 = 4.47 \times 10^{-3}$ M^{-1} s^{-1} were employed, while the values of k_2 and k_3 were systematically varied to obtain the agreement depicted in Figure 12a with $k_2 = 10^5$ s^{-1} and $k_3 = 1.5 \times 10^3$ M^{-1} s^{-1}. [A listing of the FORTRAN program is available upon request.] As a check on the internal consistency of the method, Figure 12b shows that the current dependence of the product ratio is also adequately described by the value of k_2 and k_3 obtained above in Figure 12a.[47] It is noteworthy that this value of the rate constant $k_3 = 1.5 \times 10^3$ M^{-1} s^{-1} is essentially the same as $k_3 = 1.6 \times 10^3$ M^{-1} s^{-1} obtained by Saveant's procedure (see the following section). Since magnitudes of the rate constant k_2 obtained by the two methods differ somewhat, we used the Feldberg procedure to examine the dependence of k_2 on the diffusion coefficients D. Indeed, we find that the magnitude of k_2 is sensitive to values of D, indicating that it cannot be evaluated to better than a factor of 10, in the absence of a reliable value for D(Me·).[34]

Kinetics of the Mechanism in Scheme III. Reaction Layer Method. According to the procedure developed by Saveant[32] for the mechanism in Scheme III, the product ratio R^E_{CCGE} defined in eq 48 is related to the

$$R^E_{CCGE} = 2[C_2H_6]/(2[C_2H_6] + [CH_4]) \quad (48)$$

composite kinetic parameter γ^Δ evaluated from the working curve presented in Figure 1 of ref 32. The parameter γ^Δ is related to the rate constants in Scheme III according to eq 49, where D_1 and D_2 are the

$$\gamma^\Delta = (2 \times 10^3)k_1k_2^{1/2}k_4(k_3 + k_5[XY])^{-2}(D_2/D_1^{3/2}) \quad (49)$$

diffusion coefficients of the alkylcobalt(IV) and methyl radicals, respectively, in units of cm^2 s^{-1}. The rate constant k_1 for electrolysis is in units of mol s^{-1} cm^{-2}, k_2 and k_3 have units of s^{-1}, while k_4 and k_5 are in units of M^{-1} s^{-1}. The observed product ratios were converted to γ^Δ values, and $(\gamma^\Delta)^{-1/2}$ was plotted against the chloroform concentration, i.e., XY. The slope and intercept of this plot were used in conjunction with eq 49 to obtain $k_2 = 6.8 \times 10^5$ s^{-1} and $k_3 = 1.6 \times 10^3$ M^{-1} s^{-1}, respectively. The other input parameters were set at $k_1 = 9.9 \times 10^{-10}$ mol s^{-1} cm^{-2}, $k_4 = 5 \times 10^9$ M^{-1} s^{-1}, $k_5 = 4.47 \times 10^3$ M^{-1} s^{-1}, $D_1 = 1.4 \times 10^{-5}$ cm^2 s^{-1}, and $D_2 = 4 \times 10^{-6}$ cm^2 s^{-1}.

Linear Correlation of Homogeneous and Heterogeneous Rate Constants for Electron Transfer. According to Marcus theory, the activation free energy for homogeneous electron transfer is given by eq 50,[48] where ΔG^0,

$$\Delta G_h^* = w_h + \frac{\lambda_h}{4} + \frac{\Delta G^0}{2} \quad (50)$$

λ_h, and w_h represent the standard free energy change, the homogeneous reorganization energy, and the homogeneous work term, respectively. [For simplicity, the term which is second order in ΔG^0 has been omitted from eq 50.] According to Marcus,[48] the homogeneous reorganization energy may be approximated as the sum of the individual terms for each of the reactants, i.e.,

$$\lambda_h = \lambda_1 + \lambda_2 \quad (51)$$

The individual λ_i's correspond to the appropriate values to be used in the expression for the heterogeneous activation free energy as defined in the standard manner by eq 52 for the oxidation of species 1, i.e.,

$$\Delta G_e^*(E) = w_e + \frac{\lambda_1}{4} - \frac{n\mathcal{F}}{2}(E - E_1^0) \quad (52)$$

The combination of eq 50–52 yields:

$$\Delta G_h^* = \Delta G_e^*(E) + \frac{\lambda_2}{4} + \frac{n\mathcal{F}}{2}(E - E_2^0) + (w_h - w_e) \quad (53)$$

If the heterogeneous rate of oxidation of species 1 is measured at the standard reduction potential of species 2, eq 53 simplifies to:

$$\Delta G_h^* = \Delta G_e^*(E_2^0) + \frac{\lambda_2}{4} + (w_h - w_e) \quad (54)$$

In other words, eq 54 indicates that for a simple outer-sphere electron transfer, a plot of the activation free energy for heterogeneous electron transfer vs. the corresponding quantity for a homogeneous process would be linear with a slope of unity. Furthermore, if the homogeneous activation free energy is corrected for the reorganization energy of the oxidant (i.e., $\lambda_2/4$) as was done in this study,[23] the intercept in the plot of this correlation will correspond to the difference in the electrochemical and homogeneous work terms. The difference is expected to be small, as illustrated in Figure 7.

Acknowledgment. We wish to thank the General Medical Sciences program of the National Institutes of Health and the National Science Foundation for financial support of the research and Professor J. M. Saveant for helpful comments and a preprint of his paper.[32]

(47) It should be noted that the levels of agreement in Figure 12b would be improved by using a diffusion coefficient of 1.0×10^{-6} cm^2 s^{-1} for the methyl radical. While the rate of diffusion of alkyl radicals is known to be anomalously low and solvent dependent (see Burkhart and Wong in ref 34), we made no attempt to optimize this parameter.

(48) Marcus, R. A. *J. Phys. Chem.* **1963**, *67*, 853.